Table 2 Clinical information and summary for Tax-specific CD8$^+$ T cells in 14ACs

ID	Age	Sex	WBC (/μl)	CD4 (%)[1]	CD8 (%)[1]	HLA	Tetramer (%)[2]	Functions and phenotype of Tax-specific CD8$^+$ T-cells[3]			Ably (%)[7]	PVL[8]
								IFN-γ$^+$ (%)[4]	CFSE^{low} (%)[5]	PD-1$^+$ (%)[6]		
#217	70s	F	6800	ND[9]	5.72	A24	1.94	27.7	78.9	78.7	0	14
#236	30 s	F	6500	ND	11.9	A24	2.54	31.1	0	54.1	0	22
#238	60 s	F	5700	ND	12.7	A11	1.29	36.4	100	0	0	2
#243	50 s	F	4100	ND	24.6	A2/24	0.39/3.67	11.3	27.6	93.8	0	3
#245	40 s	F	5000	ND	22.6	A2	0.73	62.5	75	ND	1	58
#251	60 s	M	4800	ND	11.9	A2/11	0.70/8.23	35.8	84.4	36.7	0	2
#279	40 s	M	6200	34.1	11.6	A2/24	4.70/0.18	12.9	30.8	70.2	1	48
#287	70 s	M	4800	72.5	10.0	A2/24	1.17/0.23	11.1	0	55.6	2	81
#309	60 s	F	4600	37.5	24.8	A11/24	6.88/4.26	51.7	76.2	85.3	1.5	29
#311	60 s	F	3200	30.6	14.8	A2/24	1.02/1.94	51.3	ND	ND	0	6
#312	50 s	F	2700	27.3	36.4	A24	2.03	77.8	ND	ND	ND	UN[10]
#313	60 s	M	7300	25.4	31.0	A24	1.11	55.7	60	90.6	ND	4
#315	50 s	F	7500	26.5	7.9	A2/24	6.88/0	24.5	84.7	20	0.6	17
#360	50 s	M	6200	37.7	29.9	A2	2.6	63.1	68.4	10.2	0	UN

[1]The number indicates percentage of CD4$^+$ or CD8$^+$ T cells in lymphocytes.

[2]The number indicates percentages of tetramer$^+$ cells in CD8$^+$ T-cells. Two numbers divided by a slash represent those detected by two different tetramers corresponding to two HLA alleles shown in the HLA column.

[3]In case of a sample carrying two of three HLA-A alleles (A2, A11, or A24), Tax-specific CTLs predominantly detected by a tetramer were used. The number represents percentage of indicated cells in the tetramer-binding CD8$^+$ T cells.

[4]Evaluated by intracellular IFN-γ staining following 6 hours stimulation with corresponding Tax peptide.

[5]Evaluated by CFSE intensities in labeled PBMC after 6 days incubation with corresponding Tax peptide stimulation.

[6]The number represents percentage of indicated PD-1$^+$Tax-specific CD8$^+$ T cells without culture.

[7]Ably; abnormal lymphocytes

[8]PVL; proviral load. The number represents copy number per 1000 PBMCs.

[9]ND; not determined

[10]UN; undetectable

specific CD8$^+$ T-cells in these ACs spontaneously proliferated without stimulation with Tax peptide, probably due to viral reactivation in HTLV-1-infected cells *in vitro*[38,39]. IFN-γ production was specifically detected for peptide stimulation, and 35.8-55.7% of Tax-specific CD8$^+$ T-cells produced a good amount of IFN-γ (mean fluorescence intensity, MFI: 63.7-195.3) upon stimulation in the samples of #251, #313, and #360. In contrast, Tax-specific CD8$^+$ T-cells in one AC (#287) did not proliferate in response to Tax peptide and showed a very weak IFN-γ response with low amounts of IFN-γ (MFI: 37.5) in a low percentage (11.1%) of Tax-specific CD8$^+$ T-cells (Figures 3A and 3B). In other ACs (#243 and #279), low frequency of IFN-γ$^+$ Tax-specific CD8$^+$ T-cells was observed, but the levels of IFN-γ production (MFI: #243; 58.8, #279; 77.6) and the proliferative responses were comparable to other ACs (Table 2). Tax-specific CD8$^+$ T-cells in #236 failed to proliferate but showed favorable IFN-γ production (MFI: 80.1) in 31.1% of the cells.

Among AC samples tested, AC#287 carried higher proviral load (81 copies in 1000 PBMCs) than any other ACs (Table 2). Since Tax-specific CD8$^+$ T-cells in #287 had severely impaired IFN-γ production and proliferative potential, we examined the relationship of the function of these T-cells with proviral loads. Both percentages of IFN-γ$^+$ and dividing Tax-specific CD8$^+$ T-cells among CD8$^+$ T-cells were likely to be inversely correlated with proviral loads although they were not statistically significant (Figure 3C and 3D). Because of the limited availability of the samples, we focused mainly on two ACs (#287 and #313) in the studies hereafter.

Dysfunction of Tax-specific CD8$^+$ T-cells and inefficient CD8$^+$ cell-mediated HTLV-1 control in AC #287

To examine whether Tax-specific CD8$^+$ T-cell responses were influenced by activation of antigen-presenting cells (APCs), PBMC from #313 (responder) and #287 (low responder) were stimulated with Tax peptide in the presence or absence of LPS, a potent activator of APCs such as dendritic cells (DCs) and monocytes/macrophages. In #313, the frequency of Tax-specific CD8$^+$ T-cells increased from 1.11% to 6.47% or 4.07% at day 13, after stimulation with or without Tax peptide, respectively. The frequency of Tax-specific CD8$^+$ T-cells in #313 further increased in the presence of Tax peptide and LPS (15.81%). In contrast to #313, the frequency of Tax-specific CD8$^+$ T-cells in #287 decreased from 1.17%

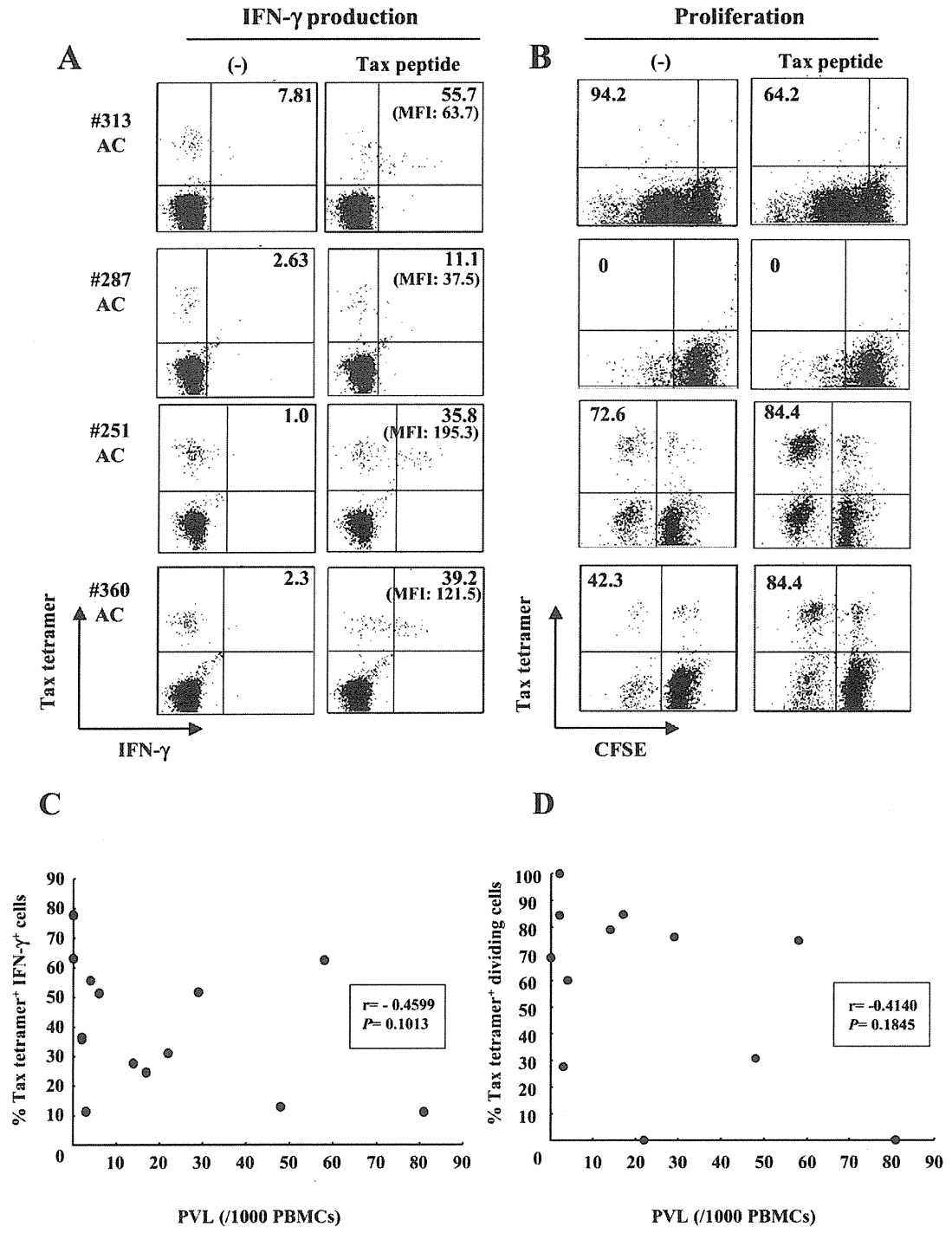

Figure 3 IFN-γ production and cell proliferation of Tax-specific CD8$^+$ T-cells in ACs. (A, B) IFN-γ production (A) and cell proliferation (B) of Tax-specific CD8$^+$ T-cells in PBMCs from 4 ACs were assessed as in Figure 2. The number given in parenthesis shows mean fluorescence intensity (MFI) of IFN-γ expression in the IFN-γ$^+$ tetramer$^+$ cells. (C, D) Relation between the percentage of IFN-γ$^+$ (C) or dividing (D) Tax-specific CD8$^+$ T-cells and proviral loads (PVL) in ACs. Dots represent individual ACs. The Spearman rank correlation test was used to determine correlations and *P* values.

to 0.2% after stimulation with Tax peptide, and was not recovered by LPS stimulation (Figure 4A). In addition, HTLV-1-infected cells have been reported to express C-C chemokine receptor type 4 (CCR4) and have FoxP3$^+$ Treg-like function[18,40]. However, the proliferative ability of Tax-specific CD8$^+$ T-cells in #287 was not restored even in the absence of CCR4$^+$ infected cells (data not shown).

To further examine the function of Tax-specific CD8$^+$ T-cells in #313 and #287, we observed the expression of CD69, an early activation marker transiently expressed on T lymphocytes that precedes cytokine secretion after antigenic stimulation, and CD107a, a marker of degranulation associated with cytotoxic activity in an antigen-specific manner[41]. CD69 was up-regulated on Tax-specific CD8$^+$ T-cells in #313 when stimulated with Tax peptide, but not in #287, which was in agreement with their abilities to produce IFN-γ (Figure 4B). In #313, 22.4% of Tax-specific CD8$^+$ T-cells mobilized CD107a to the surface during a 6-hr culture with Tax peptide stimulation, while CD107a surface expression was detected on 4% of Tax-specific CD8$^+$ T-cells in the culture without stimulation (Figure 4C). However, no CD107a mobilization was detected on the surface of Tax-specific CD8$^+$ T-cells in #287 with or without Tax peptide stimulation (Figure 4C). These results indicate that HTLV-1-specific CD8$^+$ T-cells in AC #287 did not properly activate upon antigen stimulation, and therefore failed to control HTLV-1-infected cells.

The Tax/HLA tetramers used in this study allow us to evaluate the functions of CD8$^+$ T-cells only against an immunodominant epitope, Tax. We therefore compared HTLV-1 Gag p19 in the culture between whole and CD8$^+$ cell-depleted PBMCs to examine the role of total HTLV-1-specific CD8$^+$ T-cells including the dominant Tax-specific CD8$^+$ T-cells, in suppression of HTLV-1 production from infected cells (Figure 4D). As expected, depletion of CD8$^+$ cells from PBMCs in #313 led to significantly higher HTLV-1 production compared to whole PBMCs (P = 0.0115). In contrast, HTLV-1 p19 production increased only a little in the culture of CD8$^+$ cell-depleted PBMCs in #287 (P = 0.1563), indicating that HTLV-1-specific CD8$^+$ T-cells other than the dominant Tax-specific CD8$^+$ T-cells might have a reduced ability to control the infected cells in this donor. It is of note that HTLV-1-infected cells from both two donors carried intact HTLV-1 proviral genomic DNA because HTLV-1 p19 could be detected after 7 day-culture.

Phenotypic analysis of functional and dysfunctional Tax-specific CD8$^+$ T-cells

We next characterized the differentiation status of memory T-cells in Tax-specific CD8$^+$ T-cells. Human CD8 T-cells may be classified as naïve T-cells (CD45RA$^+$CCR7$^+$CD27$^+$), T_{CM} (CD45RA$^-$CCR7$^+$CD27$^+$), T_{EM} (CD45RA$^-$CCR7$^-$CD27$^+$), and T_{Diff} (CD45RA$^+$CCR7$^-$CD27$^-$) cells[42-44]. As shown in Figure 5A, almost all Tax-specific CD8$^+$ T-cells in both #313 and #287 were skewed to CD45RA$^-$CCR7$^-$CD27$^+$ T_{EM} cells, and there was no essential difference between two donors.

A previous report has shown that PD-1 was highly up-regulated on Tax-specific CD8$^+$ T-cells in ATL patients and ACs[32]. We therefore examined PD-1 expression on Tax-specific CD8$^+$ T-cells in several AC samples, including #287. The frequency of PD-1$^+$ Tax-specific CD8$^+$ T-cells was very high in #309 (85.3%) and #313 (96%) (Figure 5B and Table 2) while those Tax-specific CD8$^+$ T-cells retained the proliferative and the cytokine-producing abilities (Figure 3A and Table 2). In #287, the frequency of PD-1-expressing Tax-specific CD8$^+$ T-cells (55.6%) was lower than #309 and #313, but higher than that of PD-1$^+$ CMVpp65-specific CD8$^+$ T-cells in the same donor (Figure 5B). The levels of PD-1 expression showed a similar tendency to the frequency of PD-1$^+$ T-cells. In addition, the blockade of PD-1/PD-ligand 1 (PD-L1) pathway did not restore the proliferative capacity of Tax-specific CD8$^+$ T-cells in #287 (data not shown).

Conserved functions of CMV-specific CD8$^+$ T-cells in #287

We next examined whether the impairment of proliferative capacity and effector functions observed in #287 CD8$^+$ T-cells were specific for HTLV-1 antigens or the result of general immune suppression. PBMC from #287 contained CMVpp65-specific CD8$^+$ T-cells (2.3% of CD8$^+$ T-cells), as detected by tetramer staining. The frequency of CMVpp65-specific CD8$^+$ T-cells increased from 2.3% to 66.0% following in vitro CMVpp65 peptide stimulation, but not without the peptide stimulation (Figure 6A). Antigen-specific IFN-γ and CD69 expression were clearly detected in CMVpp65-specific CD8$^+$ T-cells in #287 (Figures 6B and 6C). Furthermore, CMVpp65-specific CD8$^+$ T-cells mobilized CD107a to the surface in response to CMVpp65 peptide (Figure 6D). These results demonstrate that in #287, CMVpp65-specific CD8$^+$ T-cells, but not Tax-specific CD8$^+$ T-cells, have proliferative potential and effector functions, such as cytotoxic activity and IFN-γ release, suggesting that the impaired CD8$^+$ T-cell function in #287 was specific for HTLV-1.

Dysfunction of Tax-specific but not CMVpp65-specific CD8$^+$ T-cells also in sATL patients

Finally, we extended the study to see whether patients with early stage ATL might exhibit similar dysfunction selective for HTLV-1-specific CD8$^+$ T-cells. We found two smoldering ATL (sATL) patients (#110 and #353)

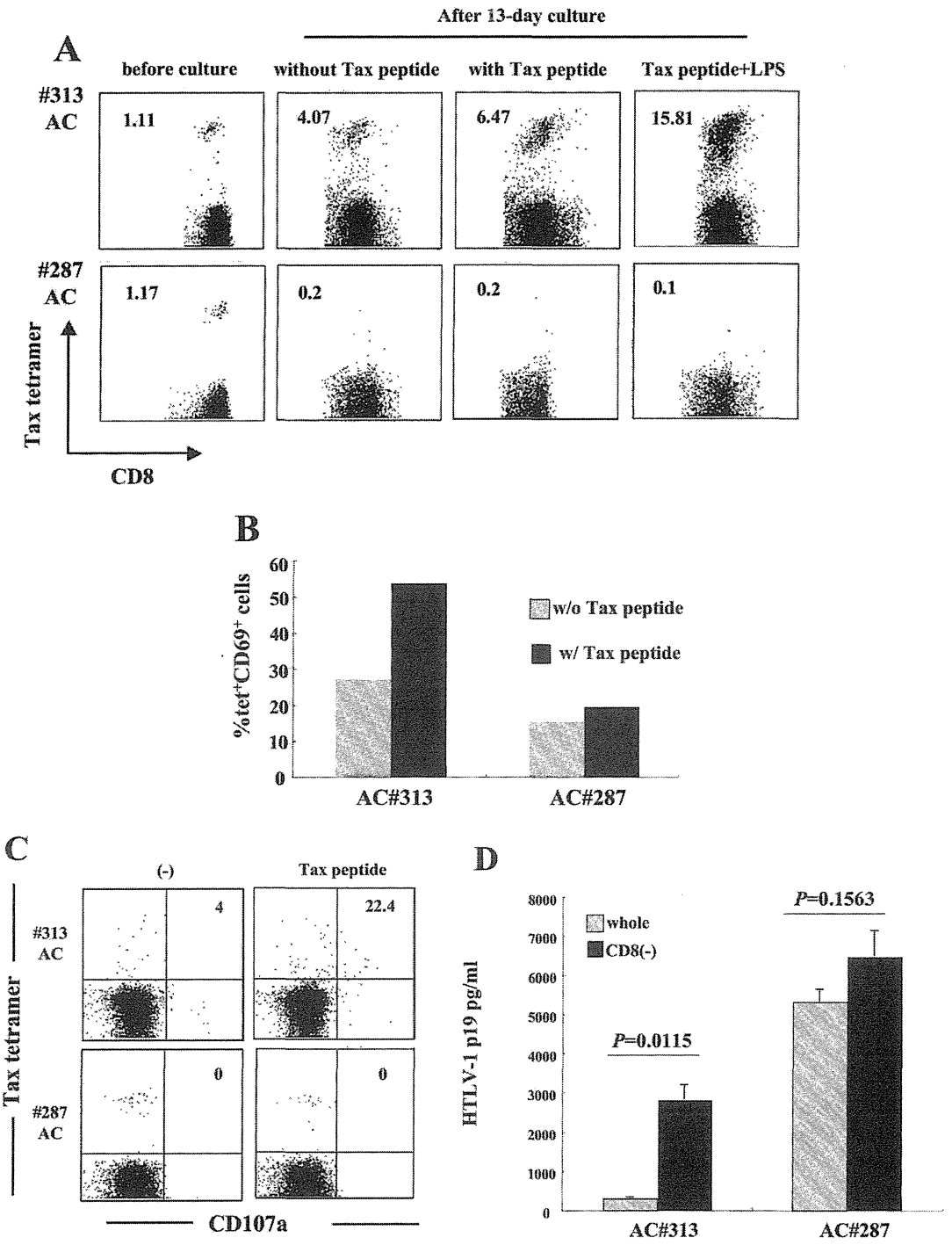

Figure 4 Dysfunction of Tax-specific CD8$^+$ T-cells and inefficient CD8$^+$ cell-mediated HTLV-1 control in AC#287. (A) For antigen-specific T-cell proliferation, PBMCs from #313 and #287 were cultured for 13 days with or without Tax peptide in the presence or absence of 0.1 μg/ml LPS. The number indicates the percentage of tetramer$^+$ cells in CD8$^+$ T-cells. (B, C) PBMCs were stimulated with or without 10 μM Tax peptide for 6 hrs. The expression of CD69 (B) and CD107a (C) in Tax-specific CD8$^+$ T-cells was analyzed by flow cytometry. (B) Bar indicates the percentage of CD69$^+$ cells in Tax-specific CD8$^+$ T-cells. (C) The number represents the percentage of CD107a$^+$ cells in Tax-specific CD8$^+$ T-cells. (D) Whole PBMCs and CD8-depleted fractions in ACs (#287 and #313) were cultured for 7 days and HTLV-1 p19 in the supernatants were measured by HTLV-1 p19 ELISA. *P* value was determined by the unpaired *t* test.

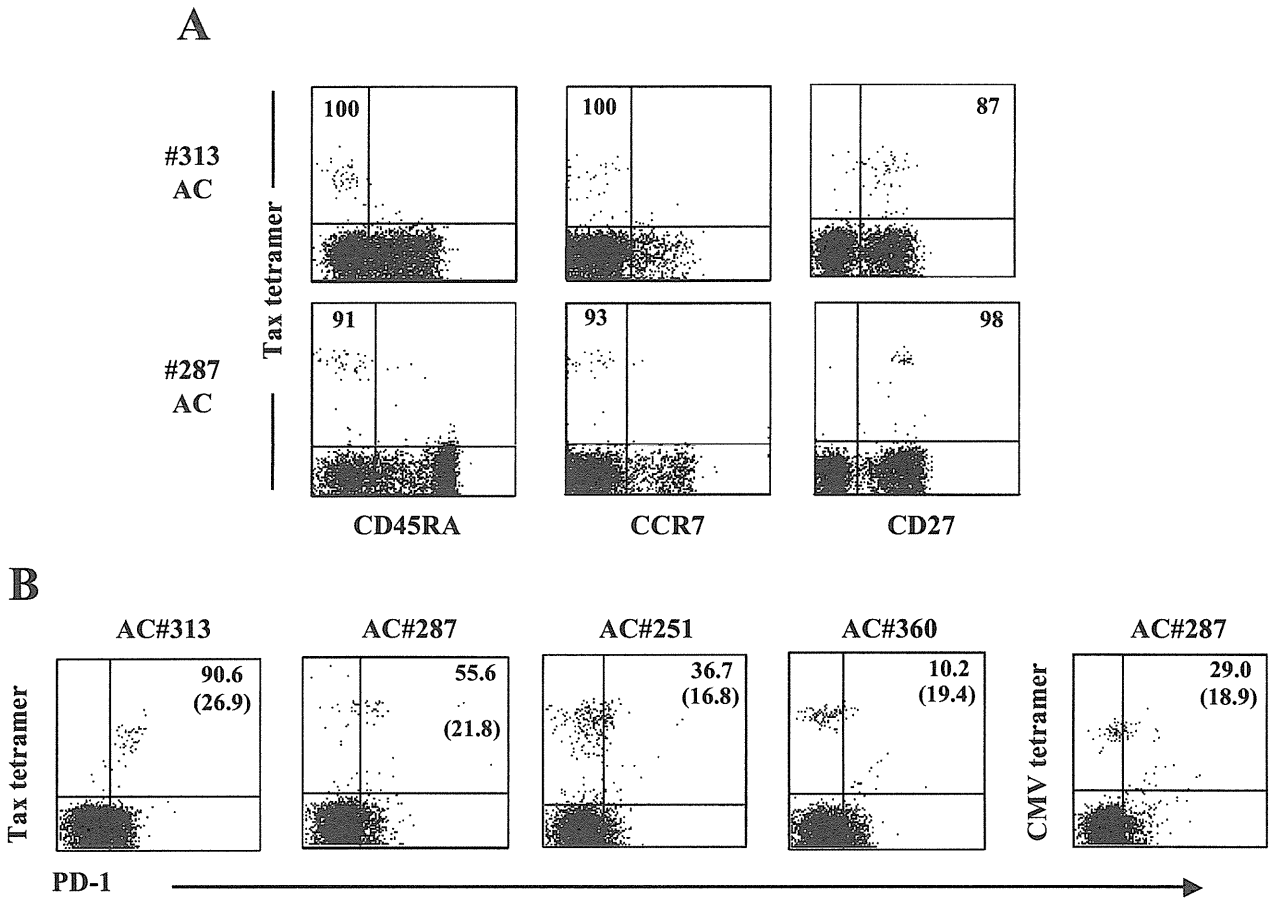

Figure 5 Phenotypic analysis of functional and dysfunctional Tax-specific CD8$^+$ T-cells. (A) Differentiation memory phenotype, based on the expression of CD45RA, CCR7, and CD27 and (B) PD-1 expression of Tax-specific CD8$^+$ T-cells from ACs were examined by flow cytometry. The number represents the percentage of indicated marker-positive or -negative cells in tetramer$^+$ CD8$^+$ T-cells. The number given in parenthesis shows MFI of PD-1 expression on the PD-1$^+$ tetramer$^+$ cells.

possessing 6.89% and 3.15% of tetramer-binding Tax-specific CD8$^+$ T-cells, respectively. The sATL patient #353 carried 5% of abnormal lymphocytes (ably) with a normal range of lymphocyte number, whose status is very close to the borderline with ACs. Patient #110 carried 4% of abnormal lymphocytes with mild lymphocytosis. Tax-specific CD8$^+$ T-cells of two sATL patients (#110 and #353) did not proliferate in response to Tax peptides as similarly observed in a cATL patient (#224) (Figure 7A) and most other cATL patients (Figure 2A and Additional file 1). In contrast, CMVpp65-specific CD8$^+$ T-cells in both sATL patients vigorously proliferated when stimulated with CMVpp65 peptides. CMVpp65-specific CD8$^+$ T-cells in a cATL (#224) also proliferated, but to a lesser degree, which might reflect general immune suppression in this patient (Figure 7).

Discussion

In this study, we detected Tax-specific CD8$^+$ T-cells in 87%, but not the rest of ACs tested, by using tetramers containing Tax major epitope-peptides presented by HLA-A*0201, A*1101, and A*2402. Tax-specific CD8$^+$ T-cells were also detected in 38% of cATL patients, but at reduced frequencies and with severely impaired functions. Further analysis of Tax-specific CD8$^+$ T-cells in 14 ACs indicated that they were functional in most of ACs tested except one (#287), whose Tax-specific CD8$^+$ T-cells poorly responded to specific peptides. However, CMVpp65-specific CD8$^+$ T-cells of this individual were fully functional. Similar T-cell dysfunction selective for HTLV-1, but not CMV, was also observed in sATL patients, one of which (#353) had no clinical symptoms but 5% abnormal lymphocytes. General immune suppression might partly account for the scarcity and/or the dysfunction of Tax-specific CD8$^+$ T-cells in ATL patients, but not those in the AC or the sATL patients as they were selective for HTLV-1. These findings suggest that HTLV-1-specific immune suppression is undergoing in a minor group of ACs and an early stage of ATL.

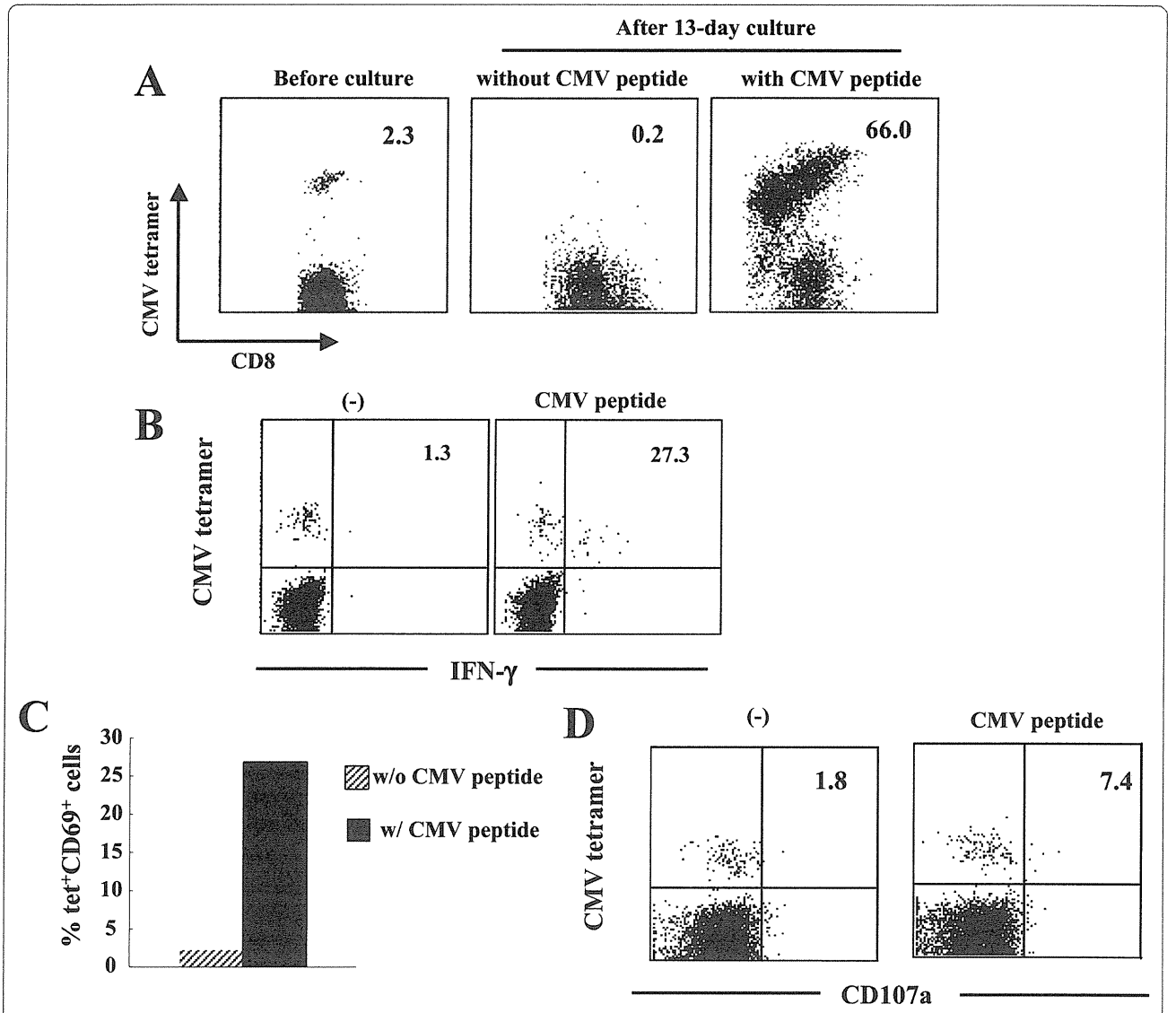

Figure 6 Conserved functions of CMV-specific CD8$^+$ T-cells in AC#287. (A) For antigen-specific T-cell proliferation, PBMCs from #287 were cultured for 13 days with or without 100 nM CMV peptide. The number indicates the percentage of CMV tetramer$^+$ cells in CD8$^+$ T-cells. (B-D) PBMCs were stimulated with or without 10 μM CMV peptide for 6 hrs. IFN-γ production (B), CD69 (C) and CD107a (D) expression of CMVpp65-specific CD8$^+$ T-cells in #287 was analyzed by flow cytometry. (B, D) The number represents the percentage of the indicated marker-positive cells in CMVpp65-specific CD8$^+$ T-cells. (C) Bar indicates the percentage of CD69$^+$ cells in CMV-specific CD8$^+$ T-cells.

The presence of tetramer-binding Tax-specific CD8$^+$ T-cells in cATL patients, although at low frequencies, implies that they have encountered antigen during the chronic phase of ATL disease, suggesting that Tax may be expressed *in vivo*. This may be supported by a previous report showing that virus-specific CD8$^+$ T-cells fails to acquire memory T-cell property of long-term antigen-independent persistence during chronic lymphocytic choriomeningitis virus (LCMV) infection[45]. However, there is no direct evidence that infected cells produce Tax in infected individuals. HTLV-1-specific T-cell responses in cATL patients are largely different from HAM/TSP patients. In HAM/TSP patients, Tax-specific CD8$^+$ T-cells proliferated vigorously and a large population of them produced IFN-γ. In contrast, the function of Tax-specific CD8$^+$ T-cells in cATL patients was profoundly suppressed, similarly to tumor infiltrating lymphocytes (TIL)[46]. In cATL patients, Tax-specific CD8$^+$ T-cells that were detected before culture decreased in number to undetectable or very low levels after 6 days, regardless of peptide stimulation (data not shown). This is not likely to be due to TCR down-regulation, because TCRs on Tax-specific CD8$^+$ T-cells in HAM/TSP patients are down-regulated on days 1 to 4

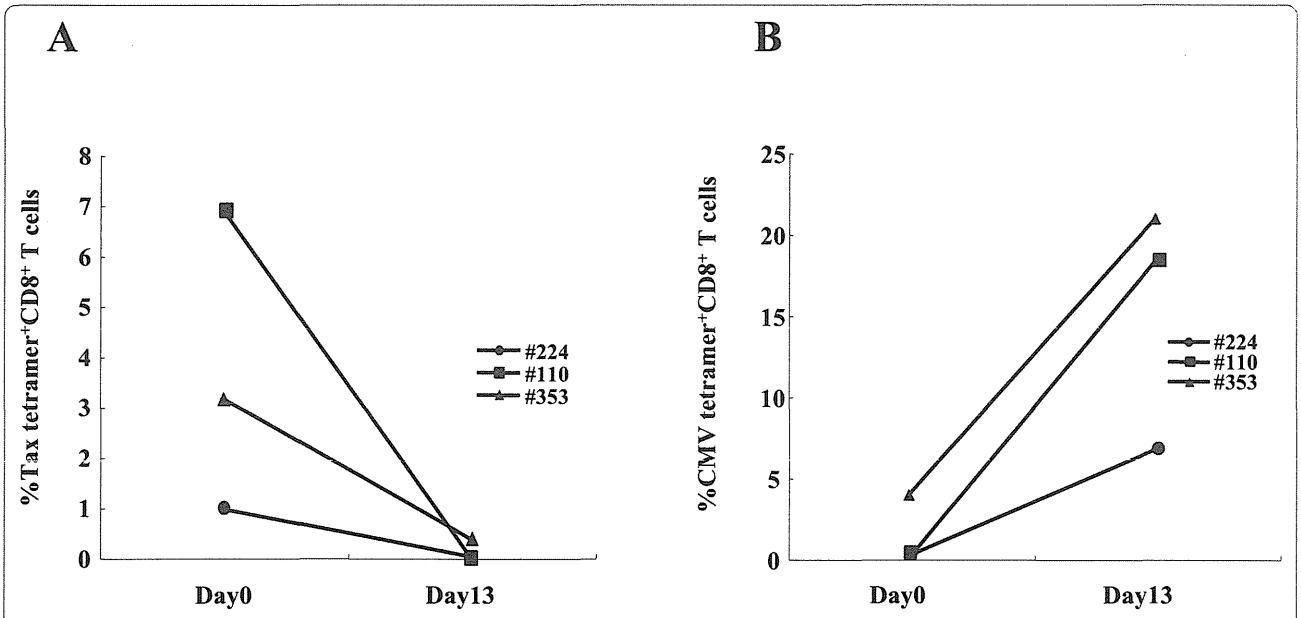

Figure 7 Impaired proliferation of Tax-specific but not CMVpp65-specific CD8$^+$ T-cells in sATL patients. For antigen-specific T-cell proliferation, PBMCs from sATL (#110; square, #353; triangle) and cATL (#224; circle) patients were cultured for 13 days with 100 nM Tax (A) or CMV (B) peptide. Each dot indicates the percentage of tetramer$^+$ cells in CD8$^+$ T-cells at day 0 and day 13 after culture. Clinical information on ATL patients used here is as follows; sATL#110: age; 40 s, gender; F, WBC#; 11,000/μL {lymphocyte (lym); 39%, abnormal lymphocytes (ably); 4%}, cATL#224: age; 50 s, gender; F, WBC#; 7900/μL (lym; 30%, ably; 33%), sATL#353: age; 60 s, gender; M, WBC#; 4620/μL (lym; 39%, ably; 5%).

and reappeared by day 6 in vitro[34]. Moreover, we could not observe any tetramer$^+$ CD8$^+$ T-cells even in the 13-day culture (data not shown), suggesting these cells might have died during the culture.

Severe dysfunction of Tax-specific CD8$^+$ T-cells was observed not only in cATL patients, but also in an AC #287. Fresh PBMCs of #287 contained 1.17% tetramer$^+$ cells in the CD8$^+$ T-cell fraction. However, none of these tetramer-positive T-cells proliferated in culture, with or without Tax peptide stimulation (Figure 3B). Although a few populations of them (11.1%) produced a small amount of IFN-γ, they lacked degranulation activity for cytotoxicity or expression of CD69, an early activation marker, upon specific stimulation (Figures 3 and 4). Importantly, CMVpp65-specific CD8$^+$ T-cells in the same donor were clearly activated, and exhibited these characteristics upon stimulation with pp65 peptides (Figure 6). These observations indicated that the impaired Tax-specific CD8$^+$ T-cells function in #287 was not attributable to general immune suppression, but to an HTLV-1-specific phenomenon. In addition, CD8-depletion study indicated that not only the dominant Tax-specific CD8$^+$ T-cell function but also other HTLV-1-specific CD8$^+$ T cell responses might be reduced in #287 (Figure 4D). Since CMV-specific CD8$^+$ T-cells responded well to the specific peptides, antigen-presenting cells in culture were not likely to be responsible for the selective suppression of Tax-specific CD8$^+$ T-cells. In addition, it has been shown that HTLV-1-infected cells generally express CCR4 and have Treg-like function[18,40]. However, depletion of CCR4$^+$ cells did not restore the proliferative ability of Tax-specific CD8$^+$ T-cells (data not shown), indicating that suppression of the infected cells were not likely to be the major reason for the impaired Tax-specific CD8$^+$ T-cell function in our culture system. These observations suggest that in #287, Tax-specific CD8$^+$ T-cells themselves might lose their functions.

Many chronic viral infections affect the phenotype, function, and maintenance of memory T-cells [24,42,47,48]. T_{EM} cells predominate in infections in which relatively high levels of antigen persist and continuous antigen stimulation are required for maintenance of T_{EM} cells. As described in HAM/TSP patients [34], Tax-specific CD8$^+$ T-cells in both ACs (#287 and #313) were primarily enriched in T_{EM} memory pool in spite of the functionality of Tax-specific CD8$^+$ T-cells (Figure 5A), which may support continuous or periodical expression of viral antigen in vivo during an asymptomatic stage.

PD-1 is known to play a major role in regulating T-cell exhaustion during chronic infection. In this study, we could not obtain any data supporting the involvement of PD-1 in the dysfunction of Tax-specific CD8$^+$ T-cells. However, we observed that Tax-specific CD8$^+$ T-cells in some ACs showed IFN-γ production, but not

proliferative capacity (Table 2). This partially lacked function of Tax-specific CD8$^+$ T-cells is similar to the features of T-cell exhaustion. Whether Tax-specific CD8$^+$ T-cells are exhausted in HTLV-1 infection, and whether other molecules associated with T-cell exhaustion are involved in the impairment of Tax-specific CD8$^+$ T-cell responses are necessary to be clarified because some inhibitory molecules such as T-cell immunoglobulin and mucin domain-containing protein-3 (TIM-3), lymphocyte activated gene-3 (LAG-3), and transcription factors including BLIMP-1 are also found to be associated with T-cell exhaustion [49].

The incidence of Tax-specific CD8$^+$ T-cell detection was high (87.0%) in ACs. Given the fact that the incidence of Tax-specific CD8$^+$ T-cells in HAM/TSP patients was 100%, a small fraction of ACs lacking detectable tetramer-binding cells might lack Tax-specific T-cell responses. Our previous study investigating GST-Tax protein-based T-cell responses supports this notion [20]. In the present study, even in ACs possessing Tax-specific CD8$^+$ T-cells, at least one individual exhibited T-cell dysfunction selectively for HTLV-1. The incidence of tetramer-positive cells was reduced in ATL patients (38.1%), and the function of these cells was impaired in all the ATL patients even with detectable tetramer-binding Tax-specific CD8$^+$ T-cells. Our findings suggest that HTLV-1-specific T-cell responses are selectively impaired in a small percentage of HTLV-1-infected individuals in the asymptomatic stages, and the proportion of individuals with such characteristics increase as the stages proceed towards ATL. Strategies to reactivate HTLV-1-specific T-cells at early stages might contribute to a reduction in the immunological risk of ATL.

Conclusions

Tax-specific CD8$^+$ T-cells were scarce and dysfunctional in a limited AC population and ATL patients, and the dysfunction of CD8$^+$ T-cells was selective for HTLV-1 in early stages. These results implied the presence of some HTLV-1-specific T-cell suppressive mechanisms even in asymptomatic stages, which are not a result of general immune suppression in ATL but could be underlying conditions toward disease progression.

Methods

Samples

Blood samples from 64 HTLV-1-seropositive individuals were used in this study: 23 asymptomatic carriers (ACs), 18 HAM/TSP patients, 2 smoldering type ATL (sATL) patients, and 21 chronic type ATL (cATL) patients. All blood samples were obtained following written informed consent, and this study was reviewed and approved by the Institutional Review Board of the Tokyo Medical and Dental University.

Peptides

Peptides used in this study were HLA-A2-restricted CTL epitopes (Tax11-19, LLFGYPVYV)[12] (Hokudo Co., Hokkaido, Japan) and (CMV495-503, NLVPMVATV)[50] (Sigma Aldrich St. Louis, MO), HLA-A11-restricted CTL epitope (Tax88-96, KVLTPPITH)[36] (Hokudo Co) and HLA-A24-restricted CTLs epitopes (Tax301-309, SFHSLHLF)[35] (Hokudo Co) and (CMV341-349, QYDPVAALF)[51] (Sigma Aldrich).

Cell Surface staining

To select samples carrying HLA-A2, -A11, or -A24, whole blood was screened with antibodies for HLA-A2, -A11, and -A24 subtypes (One Lambda, Inc., Los Angeles, CA). FITC-conjugated goat anti-mouse Ig (G+M) (Beckman Coulter Inc., Webster, TX) was used as a secondary antibody. For cell surface staining, whole blood samples were stained with the following fluorochrome-conjugated mouse anti-human mAbs; CD3-FITC, CD8-PE/Cy5, CD8-PerCP/Cy5.5 (RPA-T8, BioLegend), CD27-FITC (O323, BioLegend) CD45RA-FITC (HI 100, BD Biosciences), CD45RA-APC (HI 100, BioLegend), CD69-FITC (FN 50, BioLegend), PD-1-FITC (EH12.2H7, BioLegend), CCR7 (TG8/CCR7, Biolegend).

Tetramer staining

PE-conjugated HLA-A*0201/Tax11-19, HLA-A*1101/Tax88-96, HLA-A*2402/Tax301-309, HLA-A*0201/CMVpp65, HLA-A*2402/CMVpp65 tetramers were purchased from MBL (Nagoya, Japan). Whole blood samples or peripheral blood mononuclear cells (PBMCs) were stained with PE-conjugated Tax/HLA tetramer in conjunction with FITC-conjugated anti-CD3 (UCHT1, BioLegend San Diego, CA), and PE-Cy5-conjugated anti-CD8 monoclonal antibodies (mAbs) (HIT8a, BD Biosciences San Jose, CA). Whole blood samples were lysed and fixed in BD FACS lysing solution (BD Biosciences) before washing the cells. Samples were analyzed on a FACSCalibur (Becton Dickinson, San Jose, CA) and data analyses were performed using CellQuest software (Becton Dickinson).

Tetramer-based IFN-γ flow cytometry

Tetramer-based intracellular IFN-γ flow cytometry was performed as described previously[17], with slight modifications. In brief, PBMCs (2.0×10^5 cells) were incubated with HLA tetramer-PE and anti-CD8-PE/Cy5, washed, and stimulated with 10 μM antigenic peptide for 6 hrs at 37°C in the presence of brefeldin A (BFA, 10 μg/ml; Sigma Aldrich). The cells were stained with a

tetramer, permeabilized, and stained with anti-human IFN-γ-FITC (4S.B3, BD Biosciences).

T-cell proliferation

PBMCs (2.0-5.0 × 10^5 cells/well) labeled with carboxyfluorescein succinimidyl ester (CFSE; Sigma Aldrich) were cultured for 6 days with or without 100 nM antigenic peptide and then stained with Tax/HLA tetramer-PE and anti-CD8-PE/Cy5. In some experiments, PBMCs (2.0 × 10^5 cells) were cultured for 13 days with 100 nM antigenic peptide and 10 U/ml recombinant human IL-2 (IL-2; Shionogi, Osaka, Japan) in the presence or absence of 0.1 μg/ml Lipopolysaccharide (LPS; Sigma Aldrich). The cells were then stained with HLA tetramer-PE, anti-CD8-PE/Cy5 and anti-CD3-FITC, and analyzed by flow cytometry.

Quantification of HTLV-1 proviral load

The HTLV-1 proviral load was measured using LightCycler DNA Master SYBR Green 1 (Roche, Mannheim, Germany) with a LightCycler (Roche). Genomic DNA was extracted from PBMCs (2 × 10^6 cells) using DNeasy Blood & Tissue kits (QIAGEN, Courtaboeuf, France). The primer sets used in this study were as follows: pX2 (5'-CGGATACCCAGTCTACGTGTTTGGAGACTGT-3') and pX3 (5'-GAGCCGATAACGCGTCCATCGATGG GGTCC-3') for HTLV-1 pX, and B-globin (5'-ACACAACTGTGTTCACTAGC-3') and aB-globin (5'-CAACTTCATCCACGTTCACC-3') for β-globin. The proviral load was calculated as: [(copy number of pX)/(copy number of β-globin/2)] × 1000. HTLV-1 proviral loads in some of the PBMC samples were measured by the Group of Joint Study on Predisponsing Factors of ATL Development (JSPFAD, Japan) as described previously [20].

CD107a mobilization assay

PBMCs were stained with Tax/HLA tetramers-PE and anti-CD8-PE/Cy5, washed, and stimulated with 10 μM antigenic peptide for 6 hrs at 37°C in the presence of mouse anti-human CD107a-PerCP/Cy5.5 (H4A3, Biolegend) or mouse IgG_1-PerCP/Cy5.5 (MOPC-21, Biolegend). BFA (10 μg/ml) was added 1 hr after incubation was started. The cells were then collected and stained with an HLA tetramer.

Depletion of $CD8^+$ cells and Detection of HTLV-1 p19

$CD8^+$ cells were depleted from PBMCs by negative selection using 10-fold numbers of Dynabeads M-450 CD8 (Invitrogen, Carlsbad, CA), according to the manufacturer's instructions. The PBMCs were adjust to 1 × 10^6 cells/ml before depletion, and the resulting $CD8^+$ cell-depleted fractions were resuspended in medium with the same initial volume, irrespective of the remaining cell number. PBMCs (1 × 10^6 cells/ml) and $CD8^+$ cell-depleted PBMCs were cultured for 7 days. HTLV-1 p19 in the supernatants of those PBMCs were measured by HTLV p19 antigen ELISA (RETRO tek, Buffalo, NY).

Statistics

The Mann-Whitney U-test, the unpaired t test, and the Spearman rank correlation test were performed for statistical significance by using the Graphpad Prism software (Graphpad Software). In all cases, two-tailed *P* values less than 0.05 were considered significant.

Additional material

Additional file 1: Tax-specific $CD8^+$ T-cells in cATL patients could not proliferate against Tax-peptide stimulation. (A) CFSE-labeled PBMCs were cultured with or without 100 nM Tax-peptide for 6 days. The number indicates the percentage of $tetramer^+$ cells in $CD8^+$ T cells (Day 0) or the percentage of dividing ($CFSE^{low}$) cells in Tax-specific $CD8^+$ T-cells (Day 6). In a cATL sample #54, CFSE-labeled PBMCs were cultured in the presence of mouse IgG for other experiment. (B) PBMCs (#224) and CCR4-depleted PBMCs (#280) were cultured for 13 days in the presence of 100 nM Tax-peptide. The number indicates the percentage of $tetramer^+$ cells in $CD8^+$ T-cells.

Acknowledgments and Funding

This work was supported by a grant from the Ministry of Education, Culture, Sports, Science and Technology in Japan, and a grant for an anticancer project from the Ministry of Health, Labour, and Welfare in Japan.

Author details

[1]Department of Immunotherapeutics, Tokyo Medical and Dental University, Tokyo, Japan. [2]Department of Hematology, Imamura Bun-in Hospital, Kagoshima, Japan. [3]Division of Hematology, Department of Internal Medicine, Kinki University School of Medicine, Osaka, Japan. [4]Department of Molecular Medical Science, Institute of Medical Science, St. Marianna University School of Medicine, Kawasaki, Japan. [5]Cancer Centre, University of the Ryukyus Hospital, Okinawa, Japan. [6]Department of Hematology, National Kyushu Cancer Center, Fukuoka, Japan. [7]Institute for Clinical Research, National Kyushu Cancer Center, Fukuoka, Japan. [8]Laboratory of Tumor Cell Biology, Department of Medical Genome Science, Graduate School of Frontier Sciences, The University of Tokyo, Tokyo, Japan. [9]Department of Hematology, Osaka Minami Medical Center, Osaka, Japan.

Authors' contributions

AT carried out immunological and virological analyses, and drafted the manuscript. AH conceived of the study, participated in its design and coordination, and drafted the manuscript. AU, YM, YY, MM, IC, NU, and JO provided clinical samples. YS, YT, AS, and NZ carried out a part of the experiments. TW provided the data on proviral load of some HTLV-1-infected individuals. TM helped to draft the manuscript. MK participated in study design and helped to draft the manuscript. All authors read and approved the final manuscript.

Competing interests

The authors declare that they have no competing interests.

Received: 16 August 2011 Accepted: 7 December 2011
Published: 7 December 2011

References

1. Hinuma Y, Nagata K, Hanaoka M, Nakai M, Matsumoto T, Kinoshita KI, Shirakawa S, Miyoshi I: **Adult T-cell leukemia: antigen in an ATL cell line**

and detection of antibodies to the antigen in human sera. *Proc Natl Acad Sci USA* 1981, **78**:6476-6480.
2. Poiesz BJ, Ruscetti FW, Gazdar AF, Bunn PA, Minna JD, Gallo RC: **Detection and isolation of type C retrovirus particles from fresh and cultured lymphocytes of a patient with cutaneous T-cell lymphoma.** *Proc Natl Acad Sci USA* 1980, **77**:7415-7419.
3. de The G, Bomford R: **An HTLV-I vaccine: why, how, for whom?** *AIDS Res Hum Retroviruses* 1993, **9**:381-386.
4. Arisawa K, Soda M, Endo S, Kurokawa K, Katamine S, Shimokawa I, Koba T, Takahashi T, Saito H, Doi H, Shirahama S: **Evaluation of adult T-cell leukemia/lymphoma incidence and its impact on non-Hodgkin lymphoma incidence in southwestern Japan.** *Int J Cancer* 2000, **85**:319-324.
5. Gessain A, Barin F, Vernant JC, Gout O, Maurs L, Calender A, de The G: **Antibodies to human T-lymphotropic virus type-I in patients with tropical spastic paraparesis.** *Lancet* 1985, **2**:407-410.
6. Osame M, Izumo S, Igata A, Matsumoto M, Matsumoto T, Sonoda S, Tara M, Shibata Y: **Blood transfusion and HTLV-I associated myelopathy.** *Lancet* 1986, **2**:104-105.
7. Tajima K: **The 4th nation-wide study of adult T-cell leukemia/lymphoma (ATL) in Japan: estimates of risk of ATL and its geographical and clinical features. The T- and B-cell Malignancy Study Group.** *Int J Cancer* 1990, **45**:237-243.
8. Uchiyama T, Yodoi J, Sagawa K, Takatsuki K, Uchino H: **Adult T-cell leukemia: clinical and hematologic features of 16 cases.** *Blood* 1977, **50**:481-492.
9. Bangham CR: **HTLV-1 infection: role of CTL efficiency.** *Blood* 2008, **112**:2176-2177.
10. Jacobson S, Shida H, McFarlin DE, Fauci AS, Koenig S: **Circulating CD8+ cytotoxic T lymphocytes specific for HTLV-I pX in patients with HTLV-I associated neurological disease.** *Nature* 1990, **348**:245-248.
11. Bieganowska K, Hollsberg P, Buckle GJ, Lim DG, Greten TF, Schneck J, Altman JD, Jacobson S, Ledis SL, Hanchard B, Chin J, Morgan O, Roth PA, Hafler DA: **Direct analysis of viral-specific CD8+ T cells with soluble HLA-A2/Tax11-19 tetramer complexes in patients with human T cell lymphotropic virus-associated myelopathy.** *J Immunol* 1999, **162**:1765-1771.
12. Kannagi M, Shida H, Igarashi H, Kuruma K, Murai H, Aono Y, Maruyama I, Osame M, Hattori T, Inoko H, *et al*: **Target epitope in the Tax protein of human T-cell leukemia virus type I recognized by class I major histocompatibility complex-restricted cytotoxic T cells.** *J Virol* 1992, **66**:2928-2933.
13. Parker CE, Daenke S, Nightingale S, Bangham CR: **Activated, HTLV-1-specific cytotoxic T-lymphocytes are found in healthy seropositives as well as in patients with tropical spastic paraparesis.** *Virology* 1992, **188**:628-636.
14. Parker CE, Nightingale S, Taylor GP, Weber J, Bangham CR: **Circulating anti-Tax cytotoxic T lymphocytes from human T-cell leukemia virus type I-infected people, with and without tropical spastic paraparesis, recognize multiple epitopes simultaneously.** *J Virol* 1994, **68**:2860-2868.
15. Uchiyama T: **Human T cell leukemia virus type I (HTLV-I) and human diseases.** *Annu Rev Immunol* 1997, **15**:15-37.
16. Arnulf B, Thorel M, Poirot Y, Tamouza R, Boulanger E, Jaccard A, Oksenhendler E, Hermine O, Pique C: **Loss of the ex vivo but not the reinducible CD8+ T-cell response to Tax in human T-cell leukemia virus type 1-infected patients with adult T-cell leukemia/lymphoma.** *Leukemia* 2004, **18**:126-132.
17. Kozako T, Arima N, Toji S, Masamoto I, Akimoto M, Hamada H, Che XF, Fujiwara H, Matsushita K, Tokunaga M, Haraguchi K, Uozumi K, Suzuki S, Takezaki T, Sonoda S: **Reduced frequency, diversity, and function of human T cell leukemia virus type 1-specific CD8+ T cell in adult T cell leukemia patients.** *J Immunol* 2006, **177**:5718-5726.
18. Chen S, Ishii N, Ine S, Ikeda S, Fujimura T, Ndhlovu LC, Soroosh P, Tada K, Harigae H, Kameoka J, Kasai N, Sasaki T, Sugamura K: **Regulatory T cell-like activity of Foxp3+ adult T cell leukemia cells.** *Int Immunol* 2006, **18**:269-277.
19. Hishizawa M, Imada K, Kitawaki T, Ueda M, Kadowaki N, Uchiyama T: **Depletion and impaired interferon-alpha-producing capacity of blood plasmacytoid dendritic cells in human T-cell leukaemia virus type I-infected individuals.** *Br J Haematol* 2004, **125**:568-575.
20. Shimizu Y, Takamori A, Utsunomiya A, Kurimura M, Yamano Y, Hishizawa M, Hasegawa A, Kondo F, Kurihara K, Harashima N, Watanabe T, Okamura J, Masuda T, Kannagi M: **Impaired Tax-specific T-cell responses with insufficient control of HTLV-1 in a subgroup of individuals at asymptomatic and smoldering stages.** *Cancer Sci* 2009, **100**:481-489.
21. Gruener NH, Lechner F, Jung MC, Diepolder H, Gerlach T, Lauer G, Walker B, Sullivan J, Phillips R, Pape GR, Klenerman P: **Sustained dysfunction of antiviral CD8+ T lymphocytes after infection with hepatitis C virus.** *J Virol* 2001, **75**:5550-5558.
22. Klenerman P, Hill A: **T cells and viral persistence: lessons from diverse infections.** *Nat Immunol* 2005, **6**:873-879.
23. Kostense S, Vandenberghe K, Joling J, Van Baarle D, Nanlohy N, Manting E, Miedema F: **Persistent numbers of tetramer+ CD8(+) T cells, but loss of interferon-gamma+ HIV-specific T cells during progression to AIDS.** *Blood* 2002, **99**:2505-2511.
24. Shankar P, Russo M, Harnisch B, Patterson M, Skolnik P, Lieberman J: **Impaired function of circulating HIV-specific CD8(+) T cells in chronic human immunodeficiency virus infection.** *Blood* 2000, **96**:3094-3101.
25. Wherry EJ, Blattman JN, Murali-Krishna K, van der Most R, Ahmed R: **Viral persistence alters CD8 T-cell immunodominance and tissue distribution and results in distinct stages of functional impairment.** *J Virol* 2003, **77**:4911-4927.
26. Zajac AJ, Blattman JN, Murali-Krishna K, Sourdive DJ, Suresh M, Altman JD, Ahmed R: **Viral immune evasion due to persistence of activated T cells without effector function.** *J Exp Med* 1998, **188**:2205-2213.
27. Day CL, Kaufmann DE, Kiepiela P, Brown JA, Moodley ES, Reddy S, Mackey EW, Miller JD, Leslie AJ, DePierres C, Mncube Z, Duraiswamy J, Zhu B, Eichbaum Q, Altfeld M, Wherry EJ, Coovadia HM, Goulder PJ, Klenerman P, Ahmed R, Freeman GJ, Walker BD: **PD-1 expression on HIV-specific T cells is associated with T-cell exhaustion and disease progression.** *Nature* 2006, **443**:350-354.
28. Radziewicz H, Ibegbu CC, Fernandez ML, Workowski KA, Obideen K, Wehbi M, Hanson HL, Steinberg JP, Masopust D, Wherry EJ, Altman JD, Rouse BT, Freeman GJ, Ahmed R, Grakoui A: **Liver-infiltrating lymphocytes in chronic human hepatitis C virus infection display an exhausted phenotype with high levels of PD-1 and low levels of CD127 expression.** *J Virol* 2007, **81**:2545-2553.
29. Zhang JY, Zhang Z, Wang X, Fu JL, Yao J, Jiao Y, Chen L, Zhang H, Wei J, Jin L, Shi M, Gao GF, Wu H, Wang FS: **PD-1 up-regulation is correlated with HIV-specific memory CD8+ T-cell exhaustion in typical progressors but not in long-term nonprogressors.** *Blood* 2007, **109**:4671-4678.
30. Barber DL, Wherry EJ, Masopust D, Zhu B, Allison JP, Sharpe AH, Freeman GJ, Ahmed R: **Restoring function in exhausted CD8 T cells during chronic viral infection.** *Nature* 2006, **439**:682-687.
31. Freeman GJ, Long AJ, Iwai Y, Bourque K, Chernova T, Nishimura H, Fitz LJ, Malenkovich N, Okazaki T, Byrne MC, Horton HF, Fouser L, Carter L, Ling V, Bowman MR, Carreno BM, Collins M, Wood CR, Honjo T: **Engagement of the PD-1 immunoinhibitory receptor by a novel B7 family member leads to negative regulation of lymphocyte activation.** *J Exp Med* 2000, **192**:1027-1034.
32. Kozako T, Yoshimitsu M, Fujiwara H, Masamoto I, Horai S, White Y, Akimoto M, Suzuki S, Matsushita K, Uozumi K, Tei C, Arima N: **PD-1/PD-L1 expression in human T-cell leukemia virus type 1 carriers and adult T-cell leukemia/lymphoma patients.** *Leukemia* 2009, **23**:375-382.
33. van Lier RA, ten Berge IJ, Gamadia LE: **Human CD8(+) T-cell differentiation in response to viruses.** *Nat Rev Immunol* 2003, **3**:931-939.
34. Johnson-Nauroth JM, Graber J, Yao K, Jacobson S, Calabresi PA: **Memory lineage relationships in HTLV-1-specific CD8+ cytotoxic T cells.** *J Neuroimmunol* 2006, **176**:115-124.
35. Harashima N, Kurihara K, Utsunomiya A, Tanosaki R, Hanabuchi S, Masuda M, Ohashi T, Fukui F, Hasegawa A, Masuda T, Takaue Y, Okamura J, Kannagi M: **Graft-versus-Tax response in adult T-cell leukemia patients after hematopoietic stem cell transplantation.** *Cancer Res* 2004, **64**:391-399.
36. Harashima N, Tanosaki R, Shimizu Y, Kurihara K, Masuda T, Okamura J, Kannagi M: **Identification of two new HLA-A*1101-restricted tax epitopes recognized by cytotoxic T lymphocytes in an adult T-cell leukemia patient after hematopoietic stem cell transplantation.** *J Virol* 2005, **79**:10088-10092.
37. Elovaara I, Koenig S, Brewah AY, Woods RM, Lehky T, Jacobson S: **High human T cell lymphotropic virus type 1 (HTLV-1)-specific precursor**

cytotoxic T lymphocyte frequencies in patients with HTLV-1-associated neurological disease. *J Exp Med* 1993, **177**:1567-1573.
38. Hanon E, Hall S, Taylor GP, Saito M, Davis R, Tanaka Y, Usuku K, Osame M, Weber JN, Bangham CR: **Abundant tax protein expression in CD4+ T cells infected with human T-cell lymphotropic virus type I (HTLV-I) is prevented by cytotoxic T lymphocytes.** *Blood* 2000, **95**:1386-1392.
39. Sakai JA, Nagai M, Brennan MB, Mora CA, Jacobson S: **In vitro spontaneous lymphoproliferation in patients with human T-cell lymphotropic virus type I-associated neurologic disease: predominant expansion of CD8+ T cells.** *Blood* 2001, **98**:1506-1511.
40. Yoshie O, Fujisawa R, Nakayama T, Harasawa H, Tago H, Izawa D, Hieshima K, Tatsumi Y, Matsushima K, Hasegawa H, Kanamaru A, Kamihira S, Yamada Y: **Frequent expression of CCR4 in adult T-cell leukemia and human T-cell leukemia virus type 1-transformed T cells.** *Blood* 2002, **99**:1505-1511.
41. Betts MR, Brenchley JM, Price DA, De Rosa SC, Douek DC, Roederer M, Koup RA: **Sensitive and viable identification of antigen-specific CD8+ T cells by a flow cytometric assay for degranulation.** *J Immunol Methods* 2003, **281**:65-78.
42. Appay V, Dunbar PR, Callan M, Kienerman P, Gillespie GM, Papagno L, Ogg GS, King A, Lechner F, Spina CA, Little S, Havlir DV, Richman DD, Gruener N, Pape G, Waters A, Easterbrook P, Salio M, Cerundolo V, McMichael AJ, Rowland-Jones SL: **Memory CD8+ T cells vary in differentiation phenotype in different persistent virus infections.** *Nat Med* 2002, **8**:379-385.
43. Klebanoff CA, Gattinoni L, Restifo NP: **CD8+ T-cell memory in tumor immunology and immunotherapy.** *Immunol Rev* 2006, **211**:214-224.
44. Sallusto F, Lenig D, Forster R, Lipp M, Lanzavecchia A: **Two subsets of memory T lymphocytes with distinct homing potentials and effector functions.** *Nature* 1999, **401**:708-712.
45. Wherry EJ, Barber DL, Kaech SM, Blattman JN, Ahmed R: **Antigen-independent memory CD8 T cells do not develop during chronic viral infection.** *Proc Natl Acad Sci USA* 2004, **101**:16004-16009.
46. Radoja S, Saio M, Schaer D, Koneru M, Vukmanovic S, Frey AB: **CD8(+) tumor-infiltrating T cells are deficient in perforin-mediated cytolytic activity due to defective microtubule-organizing center mobilization and lytic granule exocytosis.** *J Immunol* 2001, **167**:5042-5051.
47. Champagne P, Ogg GS, King AS, Knabenhans C, Ellefsen K, Nobile M, Appay V, Rizzardi GP, Fleury S, Lipp M, Forster R, Rowland-Jones S, Sekaly RP, McMichael AJ, Pantaleo G: **Skewed maturation of memory HIV-specific CD8 T lymphocytes.** *Nature* 2001, **410**:106-111.
48. Penna A, Pilli M, Zerbini A, Orlandini A, Mezzadri S, Sacchelli L, Missale G, Ferrari C: **Dysfunction and functional restoration of HCV-specific CD8 responses in chronic hepatitis C virus infection.** *Hepatology* 2007, **45**:588-601.
49. Yi JS, Cox MA, Zajac AJ: **T-cell exhaustion: characteristics, causes and conversion.** *Immunology* 2010, **129**:474-481.
50. Wills MR, Carmichael AJ, Mynard K, Jin X, Weekes MP, Plachter B, Sissons JG: **The human cytotoxic T-lymphocyte (CTL) response to cytomegalovirus is dominated by structural protein pp65: frequency, specificity, and T-cell receptor usage of pp65-specific CTL.** *J Virol* 1996, **70**:7569-7579.
51. Kuzushima K, Hayashi N, Kimura H, Tsurumi T: **Efficient identification of HLA-A*2402-restricted cytomegalovirus-specific CD8(+) T-cell epitopes by a computer algorithm and an enzyme-linked immunospot assay.** *Blood* 2001, **98**:1872-1881.

doi:10.1186/1742-4690-8-100
Cite this article as: Takamori *et al.*: Functional impairment of Tax-specific but not cytomegalovirus-specific CD8$^+$ T lymphocytes in a minor population of asymptomatic human T-cell leukemia virus type 1-carriers. *Retrovirology* 2011 **8**:100.

Bone Marrow Transplantation (2011) 46, 116–118

www.nature.com/bmt

ORIGINAL ARTICLE

Long-term outcomes after hematopoietic SCT for adult T-cell leukemia/lymphoma: results of prospective trials

I Choi[1], R Tanosaki[2], N Uike[1], A Utsunomiya[3], M Tomonaga[4], M Harada[5], T Yamanaka[6], M Kannagi[7] and J Okamura[6], on behalf of the ATLL allo-HSCT Study Group

[1]*Department of Hematology, National Kyushu Cancer Center, Fukuoka, Japan;* [2]*Stem Cell Transplantation Unit, National Cancer Center Hospital, Tokyo, Japan;* [3]*Department of Hematology, Imamura Bun-in Hospital, Kagoshima, Japan;* [4]*Molecular Medicine Unit, Department of Hematology, Atomic Bomb Disease Institute, School of Medicine, Nagasaki University, Nagasaki, Japan;* [5]*Kyushu University Graduate School of Medical Sciences, Fukuoka, Japan;* [6]*National Kyushu Cancer Center, Institute for Clinical Research, Fukuoka, Japan and* [7]*Medical Research Division, Department of Immunotherapeutics, Tokyo Medical and Dental University, Tokyo, Japan*

We have previously conducted clinical trials of allogeneic hematopoietic SCT with reduced-intensity conditioning regimen (RIC) for adult T-cell leukemia/lymphoma (ATLL)—a disease caused by human T-lymphotropic virus type 1 (HTLV-1) infection and having a dismal prognosis. Long-term follow-up studies of these trials revealed that 10 of the 29 patients have survived for a median of 82 months (range, 54–100 months) after RIC, indicating a possible curability of the disease by RIC. However, we have also observed that the patterns of post-RIC changes in HTLV-1 proviral load over time among the 10 survivors were classified into three patterns. This is the first report to clarify the long-term outcomes after RIC for ATLL patients.
Bone Marrow Transplantation (2011) **46,** 116–118; doi:10.1038/bmt.2010.92; published online 19 April 2010
Keywords: adult T-cell leukemia/lymphoma; allogeneic hematopoietic SCT; reduced-intensity conditioning regimen; HTLV-1 proviral load

Introduction

Adult T-cell leukemia/lymphoma (ATLL) is a peripheral T-cell malignancy that is caused by human T-lymphotropic virus type 1 (HTLV-1) infection and commonly affects individuals at an average age of 60 years. It has been reported that the 4-year survival rate was only 10.3%; in particular, patients with an acute or lymphoma subtype showed a dismal prognosis with a 4-year survival rate of approximately 5.0%.[1] Several retrospective studies for ATLL patients younger than 50 years have suggested the possible usefulness of allogeneic hematopoietic SCT (allo-HSCT) with a conventional conditioning chemotherapy regimen. However, the treatment-related mortality by conventional allo-HSCT was high (40–60%), probably due to the disease-specific immune deficiency at diagnosis.[2–4] This unacceptable level of mortality, even in the case of young patients, critically deters the applicability of conventional allo-HSCT for the general population of ATLL.

To permit the application of allo-HSCT for ATLL in patients aged more than 50 years, we can consider allo-HSCT for ATLL conditioned with reduced-intensity regimen (hereafter, allo-HSCT conditioned with reduced-intensity regimen is referred to as 'RIC'). Few retrospective studies have reported the results of RIC for ATLL so far; Shiratori *et al.*[5] followed up 15 patients after allo-HSCT (including 10 who received RIC) whose median age was 57 years and reported that the OS rate at 3 years reached 73%. Kato *et al.*[6] investigated the results of 33 patients with allo-HSCT from unrelated donors but this study included only 6 patients receiving RIC. However, our study group had previously activated the first clinical trials of RIC in 2001. These were two trials to clarify the feasibility of RIC: one studied RIC administered with immunosuppressant antithymocyte globulin (ATG) and the other studied RIC without ATG. The results have been already published elsewhere[7,8] and the treatment-related mortality in both trials collectively decreased to the 20% level, showing that RIC is a promising procedure for ATLL patients more than 50 years of age. In this report, we present the results of long-term follow-up of the two trials and discuss the longitudinal patterns of changes in HTLV-1 proviral load in survivors.

Correspondence: Dr J Okamura, National Kyushu Cancer Center, Institute for Clinical Research, 3-1-1 Notame, Minami-ku, Fukuoka 811-1395, Japan.
E-mail: jyokamur@nk-cc.go.jp
Received 21 January 2010; revised 24 February 2010; accepted 3 March 2010; published online 19 April 2010

Patients and methods

The patient characteristics have been described in the previous reports.[7,8] Briefly, patients were eligible if they had ATLL of acute or lymphoma type and were aged between

50 and 70 years. The patients were required to be in either CR or PR at the time of trial registration, and to have a HLA-identical sibling donor. The conditioning regimen consisted of fludarabine (30 mg/m^2 per day) for 5 days and BU (1 mg/kg orally per day) for 2 days. The patients in the first study also received low-dose ATG (2.5 mg/kg per day) for 2 days, whereas those in the second study did not. On day 0, G-CSF-mobilized peripheral blood grafts from their HLA-identical sibling donors were transplanted. To prevent GVHD, we continuously infused CYA (3 mg/kg per day) starting on day −1. The degree of donor–recipient chimerism in peripheral blood mononuclear cells was examined according to the previously reported method.[9] The HTLV-1 proviral load was estimated using blood samples obtained before and at 1, 2, 3, 6, 12 months and every year after transplantation. HTLV-1 proviral DNA was measured by the quantitative PCR amplification of HTLV-1 pX DNA.[10] The detection limit of the HTLV-1 proviral load was 0.5 copies per 1000 cells. The OS curve was estimated by the Kaplan–Meier method.

Results and discussion

Long-term survivors after RIC

In all, 15 and 14 patients were registered in the first and second studies, respectively. Eleven (six and five in the first and second studies, respectively) and eight (four in each study) patients died because of ATLL and the treatment, respectively. The last treatment-related death occurred 26 months after RIC. Characteristics of the remaining 10 patients (5 in each study) are summarized in Table 1. They are currently alive with a median follow-up period of 82 months after RIC (range, 54–100 months). Of the surviving patients, six and four patients had the acute and lymphoma types of ATLL. Of 10 patients, 5 received the grafts from HTLV-1-positive sibling donors. The OS rate at 60 months (5 years) was 34% (95% confidence interval, 18–51). No death was reported beyond 36 months after RIC (Figure 1).

Of the 10 survivors, 3 developed nonhematological relapse in the skin and/or lymph nodes within a half year after RIC (Table 1). However, remission was achieved again in these patients after the discontinuation of CYA, immunosuppressive agent, and the administration of additional treatments. In one of these patients, remission was achieved with the cessation of CYA alone. Two other patients were treated with systemic chemotherapy as well as local irradiation or donor lymphocyte infusion after the discontinuation of CYA, and thereafter obtained remission. These three patients survived for 100, 88 and 54 months after RIC, respectively. Because disease recurrence is usually fatal, the clinical course for the three patients was unique. It is suggested that the newly established immunological environment after RIC might have contributed to the eradication of ATLL lesions after early relapse.

All the 10 survivors developed acute GVHD (9 grades I–II and 1 grade III). Chronic GVHD was observed in all but one patient. Although immunosuppressive treatment was discontinued in 9 of the 10 patients, 1 patient is still receiving treatment due to active chronic GVHD. The development of chronic GVHD may suggest the presence of the graft-vs-ATLL effect. Of note is that 8 of 10 survivors received RIC when they were in PR after induction chemotherapy.

Kinetic patterns of HTLV-1 proviral load in long-term survivors

Serial changes in the HTLV-1 proviral load after RIC in the 10 long-term survivors are shown in Figure 2. The changes in the proviral load are heterogeneous but can be roughly classified into three patterns. In the first pattern, the proviral load became undetectable after RIC and continued to remain so; this pattern was seen in three patients. In the second pattern, the proviral load had become undetectable but returned to detectable levels thereafter; this pattern was also seen in three patients, all of whom had received RIC from HTLV-1-negative donors. Finally, in the third pattern, the proviral load had remained at the carrier level in four patients; these patients received the grafts from donors who were HTLV-1 carriers. All the 10 survivors continue to show complete donor chimera during the observation period regardless of the HTLV-1 proviral load level.

We noted that one survivor who was donated graft from an HTLV-1 carrier showed a strikingly high proviral load (nearly 1000 copies) during the first year after RIC; this

Table 1 Characteristics of long-term survivors

Age (years)	*Gender*	*ATL subtype*	*Donor status of HTLV-1*	*Status at RIC*	*Acute GVHD*	*Chronic GVHD*	*Relapse*	*Treatment after relapse*	*Current Karnofsky PS score (%)*	*Survival after RIC (months)*
62	Male	Acute	(+)	PR	I	Yes	Lynd, skin (day 28)	d/c CsA	>90	100
66	Female	Acute	(+)	PR	II	Yes	No		>90	98
51	Male	Acute	(−)	PR	II	Yes	No		>90	98
53	Male	Lymph	(−)	PR	II	Yes	No		>90	91
54	Male	Lymph	(−)	CR	II	Yes	Lynd (day 171)	d/c CsA, Rx, Cx	>90	88
55	Male	Lymph	(+)	PR	II	Yes	No		>90	75
62	Male	Acute	(+)	CR	II	Yes	No		>90	74
50	Female	Lymph	(−)	PR	I	Yes	No		>90	62
56	Male	Acute	(−)	PR	II	Yes	Skin (day 29)	d/c CsA, DLI, steroid	>90	54
53	Female	Acute	(+)	PR	III	No	No		>90	54

Abbreviations: Cx = chemotherapy; d/c = discontinued; DLI = donor lymphocyte infusion; lynd = lymph node; PS = performance status; RIC = hematopoietic stem cell transplantation conditioned with reduced-intensity regimen; Rx = radiation therapy.

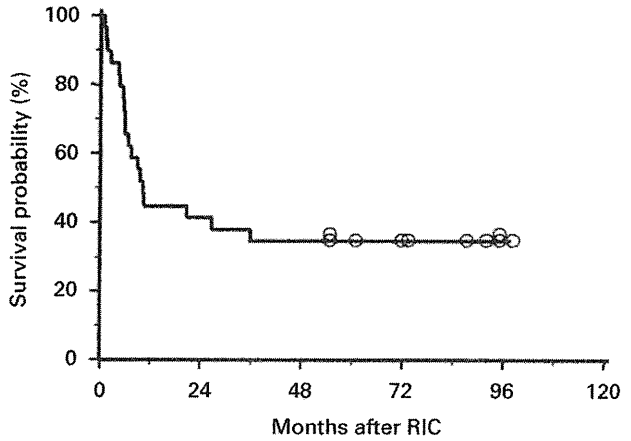

Figure 1 Kaplan–Meier curves for OS following RIC for ATLL. Circles show survivors (censored cases).

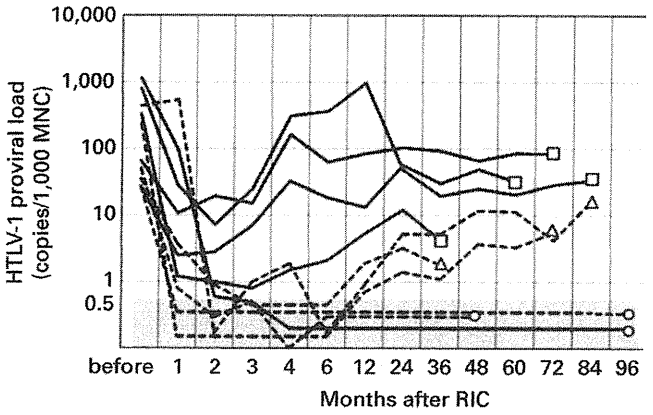

Figure 2 The longitudinal patterns of HTLV-1 proviral load after RIC in 10 long-term survivors. The HTLV-1 proviral load was measured by assaying serial blood samples after RIC by real-time PCR amplification of pX DNA and is expressed as copies per 1000 mononuclear cells (MNC). A load of less than 0.5 copies per 1000 MNC was considered undetectable, which is shown by the shaded area. A solid line indicates a patient who received a transplant from an HTLV-1 carrier donor whereas a dotted line indicates a patient from an HTLV-1-negative donor. Each circle, triangle or square indicates the latest measurement for the patient. Circle shows a pattern that the proviral load became undetectable after RIC and continued to remain so. Triangle shows a pattern that the proviral load had become undetectable but returned to detectable levels thereafter. Square shows a pattern that the proviral load had remained at the carrier level.

load then gradually decreased to the carrier level in the second year and the patient is currently surviving without any relapse. A temporary proliferation of HTLV-1-infected (nonleukemic) donor cells, as confirmed by a chimerism analysis, might have occurred due to some unknown etiology.

Conclusion

The long-term follow-up in our prospective studies has shown that one-third of the patients have survived and remain free of ATLL. We have also observed the different patterns of changes in proviral load; the pattern of changes in patients who received the grafts from HTLV-1-positive donors was different from that in patients who received the grafts from HTLV-1-negative donors. In conclusion, this is the first report on the long-term outcomes of ATLL patients who received allo-HSCT, and we have confirmed that RIC from matched sibling donors is a feasible treatment modality for ATLL, and that this treatment has a possible curative effect in patients with ATLL.

Conflict of interest

The authors declare no conflict of interest

References

1 Shimoyama M. Diagnostic criteria and classification of clinical subtypes of adult T-cell leukaemia-lymphoma. A report from the Lymphoma Study Group (1984–87). *Br J Haematol* 1991; **79**: 428–437.
2 Utsunomiya A, Miyazaki Y, Takatsuka Y, Hanada S, Uozumi K, Yashiki S *et al.* Improved outcome of adult T cell leukemia/lymphoma with allogeneic hematopoietic stem cell transplantation. *Bone Marrow Transplant* 2001; **27**: 15–20.
3 Kami M, Hamaki T, Miyakoshi S, Murashige N, Kanda Y, Tanosaki R *et al.* Allogeneic haematopoietic stem cell transplantation for the treatment of adult T-cell leukaemia/lymphoma. *Br J Haematol* 2003; **120**: 304–309.
4 Fukushima T, Miyazaki Y, Honda S, Kawano F, Moriuchi Y, Masuda M *et al.* Allogeneic hematopoietic stem cell transplantation provides sustained long-term survival for patients with adult T-cell leukemia/lymphoma. *Leukemia* 2005; **19**: 829–834.
5 Shiratori S, Yasumoto A, Tanaka J, Shigematsu A, Yamamoto S, Nishio M *et al.* A retrospective analysis of allogeneic hematopoietic stem cell transplantation for adult T cell leukemia/lymphoma (ATL): clinical impact of graft-versus-leukemia/lymphoma effect. *Biol Blood Marrow Transplant* 2008; **14**: 817–823.
6 Kato K, Kanda Y, Eto T, Muta T, Gondo H, Taniguchi S *et al.* Allogeneic bone marrow transplantation from unrelated human T-cell leukemia virus-I-negative donors for adult T-cell leukemia/lymphoma: retrospective analysis of data from the Japan Marrow Donor Program. *Biol Blood Marrow Transplant* 2007; **13**: 90–99.
7 Okamura J, Utsunomiya A, Tanosaki R, Uike N, Sonoda S, Kannagi M *et al.* Allogeneic stem-cell transplantation with reduced conditioning intensity as a novel immunotherapy and antiviral therapy for adult T-cell leukemia/lymphoma. *Blood* 2005; **105**: 4143–4145.
8 Tanosaki R, Uike N, Utsunomiya A, Saburi Y, Masuda M, Tomonaga M *et al.* Allogeneic hematopoietic stem cell transplantation using reduced-intensity conditioning for adult T cell leukemia/lymphoma: impact of antithymocyte globulin on clinical outcome. *Biol Blood Marrow Transplant* 2008; **14**: 702–708.
9 Thiede C, Florek M, Bornhauser M, Ritter M, Mohr B, Brendel C *et al.* Rapid quantification of mixed chimerism using multiplex amplification of short tandem repeat markers and fluorescence detection. *Bone Marrow Transplant* 1999; **23**: 1055–1060.
10 Sonoda J, Koriyama C, Yamamoto S, Kozako T, Li HC, Lema C *et al.* HTLV-1 provirus load in peripheral blood lymphocytes of HTLV-1 carriers is diminished by green tea drinking. *Cancer Sci* 2004; **95**: 596–601.

INFECTION AND IMMUNITY, Oct. 2011, p. 4260–4275 Vol. 79, No. 10
0019-9567/11/$12.00 doi:10.1128/IAI.05214-11

Tricomponent Immunopotentiating System as a Novel Molecular Design Strategy for Malaria Vaccine Development▽

Takeshi Miyata,[1] Tetsuya Harakuni,[1] Takafumi Tsuboi,[2,3] Jetsumon Sattabongkot,[4]†
Ayumu Ikehara,[1] Mayumi Tachibana,[5] Motomi Torii,[3,5]
Goro Matsuzaki,[1,6] and Takeshi Arakawa[1,6]*

Molecular Microbiology Group, Department of Tropical Infectious Diseases, COMB, Tropical Biosphere Research Center,[1] and Division of Host Defense and Vaccinology, Department of Microbiology, Graduate School of Medicine,[6] University of the Ryukyus, 1 Senbaru, Nishihara, Okinawa 903-0213, Cell-Free Science and Technology Research Center and Venture Business Laboratory, Ehime University, Matsuyama, Ehime 790-8577,[2] Ehime Proteo-Medicine Research Center, Ehime University,[3] and Department of Molecular Parasitology, Ehime University, Graduate School of Medicine, Shitsukawa,[5] Toon, Ehime 791-0295, Japan, and Department of Entomology, Armed Forces Research Institute of Medical Sciences, Bangkok 10400, Thailand[4]

Received 8 April 2011/Returned for modification 11 May 2011/Accepted 21 July 2011

The creation of subunit vaccines to prevent malaria infection has been hampered by the intrinsically weak immunogenicity of the recombinant antigens. We have developed a novel strategy to increase immune responses by creating genetic fusion proteins to target specific antigen-presenting cells (APCs). The fusion complex was composed of three physically linked molecular entities: (i) a vaccine antigen, (ii) a multimeric α-helical coiled-coil core, and (iii) an APC-targeting ligand linked to the core via a flexible linker. The vaccine efficacy of the tricomponent complex was evaluated using an ookinete surface protein of *Plasmodium vivax*, Pvs25, and merozoite surface protein-1 of *Plasmodium yoelii*. Immunization of mice with the tricomponent complex induced a robust antibody response and conferred substantial levels of *P. vivax* transmission blockade as evaluated by a membrane feed assay, as well as protection from lethal *P. yoelii* infection. The observed effect was strongly dependent on the presence of all three components physically integrated as a fusion complex. This system, designated the tricomponent immunopotentiating system (TIPS), onto which any recombinant protein antigens or nonproteinaceous substances could be loaded, may be a promising strategy for devising subunit vaccines or adjuvants against various infectious diseases, including malaria.

Adjuvants are defined as any substances that enhance immune responses to vaccine antigens; however, they can be categorized into targeting molecules or systems that facilitate the delivery of antigens to antigen-presenting cells (APCs) and substances that help elicit their activation (2, 11, 14, 25, 27). Adjuvants are essential components of recombinant protein-based subunit vaccines, because nonreplicating inert antigens are often weakly immunogenic when administered in the absence of extraneous adjuvants (25). Aluminum hydroxide (Alum) is the only adjuvant that has been used clinically over the past several decades (11), but recently a number of APC-activating adjuvants have been developed, and some of them have already been released to the international market (14, 27). However, no targeting molecules or systems are licensed for clinical use yet.

Dendritic cells (DCs) are considered the most effective APCs. They have highly efficient and specialized functions in the uptake and presentation of foreign antigens to T and B lymphocytes, allowing them to mount appropriate immune responses (5, 8). DCs are important initiators and modulators of immune responses, and hence, in the field of vaccine research, much attention has been focused on the APC function of DCs. However, B lymphocytes also take up foreign antigens via surface immunoglobulin (Ig) (B cell receptors [BCRs]) and present protein epitopes through the major histocompatibility complex (MHC) class II–T cell receptor interaction for antibody production (9, 10, 17, 23, 24, 33, 34). Thus, B lymphocytes are unique in that they are APCs as well as effector cells. An additional unique feature of B lymphocytes, which distinguishes them from DCs, is that they can recognize conformational epitopes (for example, those present on the surfaces of protein antigens) in addition to linear epitopes. They capture cognate antigens via specific BCRs, present linear epitopes within the captured antigen on the MHC class II molecules, and subsequently receive cognate help from T lymphocytes in the secondary lymphoid organs, such as local draining lymph nodes (10). This T-B lymphocyte interaction does not require DC involvement (26, 33). Therefore, it is theoretically plausible that targeting of the BCRs present on the surfaces of the B lymphocytes in the follicles of the draining lymph nodes by exploiting the Ig binding ligands would increase the chance that antigens would encounter cognate B lymphocytes in the follicles and would be captured and presented to T lymphocytes for efficient antibody production. By exploiting this immunological mechanism, it may be possible to augment immune responses to otherwise weakly immunogenic recombinant antigens (2).

* Corresponding author. Mailing address: Molecular Microbiology Group, Tropical Biosphere Research Center, COMB, University of the Ryukyus, 1 Senbaru, Nishihara, Okinawa 903-0213, Japan. Phone and fax: 81-98-895-8974. E-mail: tarakawa@comb.u-ryukyu.ac.jp.
† Present address: Mahidol Vivax Research Center, Faculty of Tropical Medicine, Mahidol University, Bangkok, Thailand.
▽ Published ahead of print on 1 August 2011.

TABLE 1. Sequences of oligonucleotides and a synthetic gene encoding the COMP(Gly26–Gly80) coiled-coil domain used in this study

Oligonucleotide	Sequence[a]
#1	5′-CCATGGGTAGCATTATCAACGAAACCGCCGATGATATTGTGTATCGCTTGACCGTGAT CATTGATGATCGCTATGAAAGCCTGAAAAATCTGATTACCTTACGTGCCGACCGCCTG GAAATGATTATTAATG-3′
#2	5′-CTCGAGCGGGCCCGGGCCGCTACCGCCACCGCCGTGATGATGGTGATGATGGCTACC GCCACCGCCCGGGCCCGGGCCGATGCTCGCCAAGATGGTCGAAACATTGTCATTAAT AATCATTTCCAGGCGGTC-3′
#3	5′-GTCGACGTGGATAACAAATTTAATAAAGAACAGCAGAACGCCTTCTATGAAATTCTG CATCTGCCGAACCTGAACGAAGAACAGCGTAACGCCTTTATTCAGAGCCT-3′
#4	5′-CTCGAGTTATTTCGGGGCCTGTGCATCGTTCAGTTTTTTGGCTTCTGCCAGCAGATTG GCGCTCTGGCTCGGATCATCTTTCAGGCTCTGAATAAAGGCGTTACGCT-3′
#5	5′-TCGACCATCTTGGCGTGCATCGGCCCGGGCCCG-3′
#6	5′-CGGGCCCGGGCCGATGCACGCCAAGATGGTCG-3′
#7	5′-CCGGGCCCGGGCGGTTGCGGCGGTAGCCATCATCAC-3′
#8	5′-ATGATGGCTACCGCCGCAACCGCCCGGGCCCGG-3′
#9	5′-GCGCCATGGGTGATCTGGCGCCGCAGATG-3′
#10	5′-GGCTCGAGGCCACACGCATCGCATTCCATAAC-3′
#11	5′-TCGACGGCCCGGGCCCGGGCGGTGGCGGTAGCCATCATCACCATCATCACGGCGGTG GCGGTAGCGGCCCGGGCCCGC-3′
#12	5′-TCGAGCGGGCCCGGGCCGCTACCGCCACCGCCGTGATGATGGTGATGATGGCTACCG CCACCGCCCGGGCCCGGGCCG-3′
COMP(Gly26–Gly80)	5′-GGCGGTGATCTGGCGCCGCAGATGCTGCGCGAACTGCAGGAAACCAACGCGGCCCT GCAAGATGTGCGTGAACTGCTGCGCCAGCAAGTGAAAGAAATTACCTTTCTGAAAAA TACCGTTATGGAATGCGATGCGTGTGGCATGCAGCCGGCCCGTACCCCGGGC-3′

[a] Underlined sequences represent restriction enzyme recognition sites.

It should be noted that certain anti-infectious vaccines need to rely on recombinant subunit proteins, because some infectious diseases, including malaria and other parasitic diseases, defy conventional methods of pathogen inactivation or attenuation for vaccine production; therefore, antigens derived from these pathogens need to be transformed into efficacious vaccines with the help of adjuvants (2).

In this study, we devised a new immune enhancing system for the development of malaria vaccines, and to demonstrate its efficacy, we exploited two malaria parasite antigens, the *Plasmodium vivax* ookinete surface protein (OSP) Pvs25 and *Plasmodium yoelii* merozoite surface protein-1 (MSP1), which are known to require native conformational epitopes in order to function as effective vaccines (7, 16, 31, 32). We also exploited the Z domain, a derivative of the B domain of the Ig-binding domains (IBDs) of *Staphylococcus aureus* protein A (SpA), as a targeting ligand for B lymphocytes (19). The Z domain was genetically conjugated to an α-helical coiled-coil multimer-forming domain (20) of tetrabrachion (TB) (29) or cartilage oligomeric matrix protein (COMP) (12) both to increase its structural stability and binding avidity and to facilitate receptor cross-linking. We demonstrated that antigens loaded onto these multimeric delivery complexes targeted B lymphocytes and robustly enhanced antiparasitic immunity when administered to mice through the subcutaneous (s.c.) or intranasal (i.n.) route. Furthermore, not only are all three of these components (i.e., the antigen, the core motif, and the ligand) essential, but they must also be integrated into the fusion complex for the efficient induction of an immune response.

MATERIALS AND METHODS

Construction of the TB- and COMP-based delivery molecule expression plasmids. An *Escherichia coli* codon-optimized synthetic gene encoding the TB coiled-coil domain (Gly1 to Ile52; Protein Data Bank [PDB] accession no. 1YBK) fused to a spacer sequence (see Fig. 1a, region b) was constructed by annealing two overlapping oligonucleotides (oligonucleotides #1 [sense] and #2 [antisense], containing an NcoI and an XhoI site, respectively), followed by PCR amplification using *Vent* DNA polymerase (New England BioLabs, Beverly, MA). The amplified fragment was cloned into pCR2.1 (Life Technologies, Carlsbad, CA), and then, after digestion with NcoI and XhoI, the fragment generated was subcloned into the corresponding sites in pET-21d (Merck KGaA, Darmstadt, Germany) to construct the TB-spacer (TB coiled-coil domain fused to a spacer) expression plasmid (see Fig. 1a). Similarly, a synthetic gene encoding the Z domain (Val1 to Lys58; PDB accession no. 2SPZ), a derivative of the B domain of SpA, was PCR amplified by annealing two overlapping oligonucleotides (oligonucleotides #3 [sense] and #4 [antisense], containing a SalI and an XhoI site, respectively). The amplified fragment was cloned into pCR2.1, which was then digested with SalI and XhoI, and the fragment generated was subcloned into the XhoI site on the pET-21d-TB-spacer expression plasmid to construct the TB-Z expression plasmid (Fig. 1a).

Next, to introduce a cysteine (Cys) residue into the TB-Z to construct TB-(Cys)-Z, site-directed mutagenesis was performed (QuikChange II site-directed mutagenesis kit; Agilent Technologies Inc., Wilmington, DE). TB(S52C)-Z was constructed by substituting Cys for serine 52 (Ser52) within the TB coding region (see Fig. 1a, region b) by PCR using primer set #5 (sense)–#6 (antisense) with the TB-Z expression plasmid as template DNA. Similarly, TB(C60)-Z was constructed by PCR using primer set #7 (sense)–#8 (antisense) to introduce a Cys residue immediately after Gly59 (see Fig. 1a, region b).

A gene encoding the COMP coiled-coil domain (Gly27 to Gly72; PDB accession no. 1VDF) was PCR amplified by using primer set #9 (sense)–#10 (antisense), containing an NcoI and an XhoI site, respectively, and plasmid DNA containing an *E. coli* codon-optimized synthetic gene encoding COMP(Gly26–Gly80) as the template (12). The amplified fragment was digested with NcoI and XhoI and was subcloned into the corresponding sites in pET-22b (Merck KGaA) to construct the COMP expression plasmid (see Fig. 2a). To fuse a spacer sequence to the COMP, two oligonucleotides (oligonucleotides #11 [sense] and #12 [antisense]) were annealed and inserted into a unique XhoI site in the COMP expression plasmid, constructing the COMP-spacer expression plasmid. For construction of the COMP-spacer fused to the Z domain (COMP-Z), oligonucleotides #3 and #4 were used as described above for the construction of the TB-Z expression plasmid (Fig. 2a). Table 1 lists the sequences of all the oligonucleotides and of a synthetic gene encoding the COMP(Gly26–Gly80) coiled-coil domain (12) used in this study.

Expression and purification analysis of the delivery molecules. *E. coli* BL21(DE3) was transformed with each engineered expression plasmid and was cultured in LB broth with ampicillin; then protein expression was induced by the addition of 1 mM isopropyl-β-D-thiogalactopyranoside (IPTG). After a 16-h

induction, the supernatant was collected by centrifugation (9,600 × *g*, 20 min), followed by filtration (FastCap filter; pore size, 0.2 mm; Nalgene Nunc International Inc., Rochester, NY). The supernatant was subjected to Ni-nitrilotriacetic acid (NTA) affinity chromatography (HisTrap FF [Fast Flow] columns prepacked with Ni Sepharose 6; GE Healthcare, Little Chalfont, United Kingdom).

Affinity-purified proteins were analyzed by sodium dodecyl sulfate-polyacrylamide gel electrophoresis (SDS-PAGE) or native PAGE. Proteins were transferred to a polyvinylidene difluoride (PVDF) membrane, blocked with 10% skim milk in phosphate-buffered saline (PBS), and washed with PBS-T (PBS with 0.05% Tween 20). Then the membrane was incubated with horseradish peroxidase (HRP)-conjugated goat IgG (1:4,000; Santa Cruz Biotechnology Inc., Santa Cruz, CA). Chemiluminescence was detected using the Western Lightning kit (Perkin-Elmer, Inc., Waltham, MA). Purified proteins were also analyzed by size exclusion chromatography (flow rate, 0.8 ml/min; HiLoad 16/60 Superdex 75 pg column; GE Healthcare).

Chemical conjugation of antigens to delivery molecules. Recombinant Pvs25H-A was expressed and purified as described previously (22) and was chemically conjugated to the affinity-purified TB(Cys)-Z [TB(S52C)-Z or TB(C60)-Z] or COMP-Z using the heterobifunctional cross-linker *N*-succinimidyl-3-(2-pyridyldithio)propionate (SPDP; Thermo Scientific, Inc., Rockford, IL). Six milligrams of Pvs25H-A (2 mg/ml in PBS-EDTA) was incubated with SPDP (final concentration, 0.6 mM) for 1 h at room temperature (designated Pvs25H-A^{pyr} in Fig. 3a). The reaction mixture was buffer-exchanged with PBS (Amicon Ultra-15 centrifugal filter unit; molecular weight cutoff [MWCO], 10,000; Millipore, Billerica, MA) to remove excess reagents and by-products. Concomitantly, 5 mg of the TB(Cys)-Z or COMP-Z (2 mg/ml in PBS-EDTA) was treated with dithiothreitol (DTT; 50 mM) for 30 min at 37°C and was buffer-exchanged with PBS [designated TB(Cys)-Z^{red} or COMP-Z^{red} in Fig. 3a]. Three milligrams of Pvs25H-A^{pyr} and 1 mg of TB(Cys)-Z^{red} or COMP-Z^{red} were mixed and incubated at room temperature overnight for conjugation. The conjugated sample was buffer-exchanged with PBS as before.

A 19-kDa C-terminal fragment of MSP1 (MSP1-19) of the rodent malaria parasite *P. yoelii* was loaded onto the delivery molecules using essentially the same conjugation method as that described above for the Pvs25H-A antigen.

The endotoxin levels of all of the conjugated proteins were measured (Pyrogen Single Test Vials; Cambrex, East Rutherford, NJ) prior to administration to mice, and we found that they were less than 15 pg endotoxin/μg of protein.

Ig-ELISA. A human IgG–enzyme-linked immunosorbent assay (ELISA) was conducted to analyze the tricomponent complexes. Briefly, 5 μg/ml of human IgG (Sigma-Aldrich, St. Louis, MO) diluted with bicarbonate buffer (15 mM Na_2CO_3, 35 mM $NaHCO_3$ [pH 9.6]) (50 μl/well) was used as a capture antigen for the Z domain-containing proteins; it was applied to a 96-well microtiter plate (Sumilon; Sumitomo Bakelite Co., Ltd., Tokyo, Japan) and was incubated at 4°C overnight. The plate was blocked with PBS containing 1% bovine serum albumin (BSA) for 2 h at 37°C. Samples (2 μg of total protein/well) were applied and incubated for 2 h at 37°C, followed by incubation with 5 μg/ml of human IgG for 2 h at 37°C to mask unbound free Z domains. A mouse anti-His tag antibody (1:4,000; GE Healthcare), a mouse anti-Pvs25 antiserum (1:500), or a mouse anti-MSP1-19 antiserum (1:100) was applied and incubated for 2 h at 37°C. Anti-mouse IgG conjugated to alkaline phosphatase (AP) (1:4,000; Sigma-Aldrich), followed by *p*-nitrophenylphosphate (Bio-Rad Laboratories Inc., Redmond, WA), was added and incubated for 20 min at 37°C. The optical density at 415 nm (OD_{415}) was measured using a microplate reader (Bio-Rad).

Using essentially the same human IgG-ELISA protocol as that described above, the affinity of the COMP-Z delivery molecule for various human or mouse Igs was evaluated. The Igs used as capture antigens were 5 μg/ml of human or mouse IgG (Sigma-Aldrich), 10 μg/ml of human (Sigma-Aldrich) or mouse (Bethyl Laboratories Inc., Montgomery, TX) IgM, 10 μg/ml of human or mouse IgA (Sigma-Aldrich), 10 μg/ml of human IgG1 Fab lambda or kappa (Bethyl Laboratories Inc.), or 10 μg/ml of mouse IgG Fab (Jackson ImmunoResearch Laboratories, Inc., West Grove, PA). After the plate was blocked with 1% BSA in PBS, the COMP-Z or COMP (2 μg/well each) was applied and incubated for 2 h at 37°C, followed by incubation with 5 μg/ml of human IgG for 2 h at 37°C to mask unbound free Z domains. A mouse (1:4,000; GE Healthcare) or rabbit (1:4,000; Rockland Immunochemicals, Inc., Boyertown, PA) anti-His tag antibody was applied for detection of the human or mouse Ig-bound delivery molecules, respectively. Then anti-mouse or anti-rabbit IgG conjugated to AP (1:4,000; Sigma-Aldrich), followed by its substrate, was applied for analysis.

Analysis of the target immune cells of the COMP-Z by flow cytometry. The COMP (2 mg; 62.5 nmol) or COMP-Z (2 mg; 27.6 nmol) was treated with DTT (50 mM) for 30 min at 37°C, and the buffer was replaced with PBS (Amicon Ultra-15 centrifugal filter unit; MWCO, 10,000; Millipore). The DTT-treated COMP or COMP-Z (2 mg/ml in PBS) was incubated with maleimide-polyethylene oxide (PEO_2)-biotin (final concentration, 20 mM; Thermo Scientific Inc.) for 16 h at room temperature, and the buffer was replaced with PBS as before.

Splenocytes isolated from naïve BALB/c mice were suspended in RPMI medium (Gibco Inc., Grand Island, NY) and were collected by centrifugation (377 × *g*, 10 min). Cells were incubated in red blood cell (RBC) lysis buffer (17 mM Tris buffer [pH 7.6], 140 mM NH_4Cl) for 5 min at room temperature, washed, and resuspended in RPMI medium. Cells were counted (KOVA Glasstic slide 10; Hycor Biomedical Inc., Garden Grove, CA), and the concentration was adjusted to 5 × 10^6 cells/ml with cell suspension buffer (PBS containing 2% newborn calf serum and 0.03% NaN_3). Fluorescein isothiocyanate (FITC)-conjugated antibodies to CD19 (clone 1D3), CD3e (clone 145-2C11), CD11b (clone M1/70), or CD11c (clone HL3), along with R-phycoerythrin (PE)-conjugated antibodies to Ly-6G and Ly-6C (Gr-1, clone RB6-8C5) (BD Biosciences, Sparks, MD), allophycocyanin-conjugated anti-mouse MHC class II (I-A/I-E) (eBioscience, San Diego, CA), and isotype control antibodies (BD Biosciences), were used for analysis. All antibodies were used at the concentrations recommended by the manufacturers.

Spleen cells (5 × 10^5) were first treated with a monoclonal antibody (clone 2.4G2) to block Fc receptors and were then washed, and biotinylated COMP or COMP-Z (0.31 pmol) was added to the cells and incubated. Then PE-conjugated streptavidin (BD Biosciences) was added to the cells and incubated. Cells were washed and adjusted to 1 ml with cell suspension buffer. The incubation conditions for each step were 20 min at 4°C. Data were acquired using a FACSCalibur flow cytometer and were analyzed with CellQuest software (BD Biosciences).

Immunization of mice. Seven-week-old female BALB/c or C57BL/6 mice (Japan SLC, Shizuoka, Japan), 4 to 10 per group, were immunized at weeks 0, 2, and 4 via the s.c. or i.n. route with various immunization samples. For all mouse immunization studies, 30 μg of the vaccine antigen (i.e., Pvs25H-A or MSP1-19) was administered as a conjugated or unconjugated protein. Incomplete Freund's adjuvant (IFA; Difco Laboratories, Detroit, MI), Alum (Imject Alum adjuvant; Thermo Scientific, Inc.), or cholera toxin (CT; List Biological Laboratories, Campbell, CA) was used as an s.c. or i.n. adjuvant where indicated. The endotoxin levels of all of the immunization samples were measured (Cambrex) prior to administration to mice, and we found that they were less than 15 pg endotoxin/μg of protein.

Animal experimental protocols were approved by the University of the Ryukyus Animal Care and Use Committee, and the experiments were conducted according to the institutional ethical guidelines for animal experiments.

Determination of antigen-specific serum IgG titers by ELISA. Mice were anesthetized 2 weeks after the third immunization (week 6) by intraperitoneal (i.p.) injection of pentobarbital sodium salt (Nacalai Tesque Inc., Kyoto, Japan) and were euthanized by exsanguination for the collection of antisera. For analysis of the long-term serum IgG response to the Pvs25H-A antigen, blood was collected at days 0, 14, 42, 91, 126, 196, and 273.

Antigen-specific serum antibodies were analyzed by ELISA as described previously (3, 4, 21, 22). Briefly, the ELISA plate was coated with the Pvs25H-A (5 μg/ml) or MSP1-19 (5 μg/ml) protein in bicarbonate buffer at 4°C overnight and was then blocked with 1% BSA in PBS for 2 h at 37°C. Twofold serial dilutions of the antisera, starting with a 50-fold dilution in PBS with 0.5% BSA, were applied and incubated for 2 h at 37°C. AP-conjugated anti-mouse IgG (1:4,000; Sigma-Aldrich), IgG1 (1:4,000; MP Biomedicals, Solon, OH), or IgG2a (1:4,000; MP Biomedicals) was applied and incubated for 2 h at 37°C. Then *p*-nitrophenylphosphate (Bio-Rad) was applied, and the OD_{415} was measured after 20 min of incubation at 37°C by using a microplate reader (Bio-Rad). The antibody titer was defined either as the serum dilution that gave an OD_{415} value equal to 0.1 or as the serum dilution for which a 1-magnitude-higher dilution gave an OD_{415} value less than 0.1.

Mosquito membrane feed assay and detection of native Pvs25 protein by antisera derived from immunized mice. The mosquito membrane feed assay was conducted by a method described previously (3, 4, 21, 22). Single-species infection with *P. vivax* was confirmed by Giemsa staining of thick and thin blood smears. The levels of parasitemia and gametocytemia were 0.03% and 0.002% for donor 1, 0.23% and 0.01% for donor 2, and 0.21% and 0.01% for donor 3, respectively. Native Pvs25 protein on the surfaces of *P. vivax* ookinetes was detected by immunofluorescence (21, 22) using antisera obtained from mice immunized with the tricomponent complex.

All human subject research conducted in this study was reviewed and approved by the Ethics Committee of the Thai Ministry of Public Health and the Institutional Review Board of the Walter Reed Army Institute of Research.

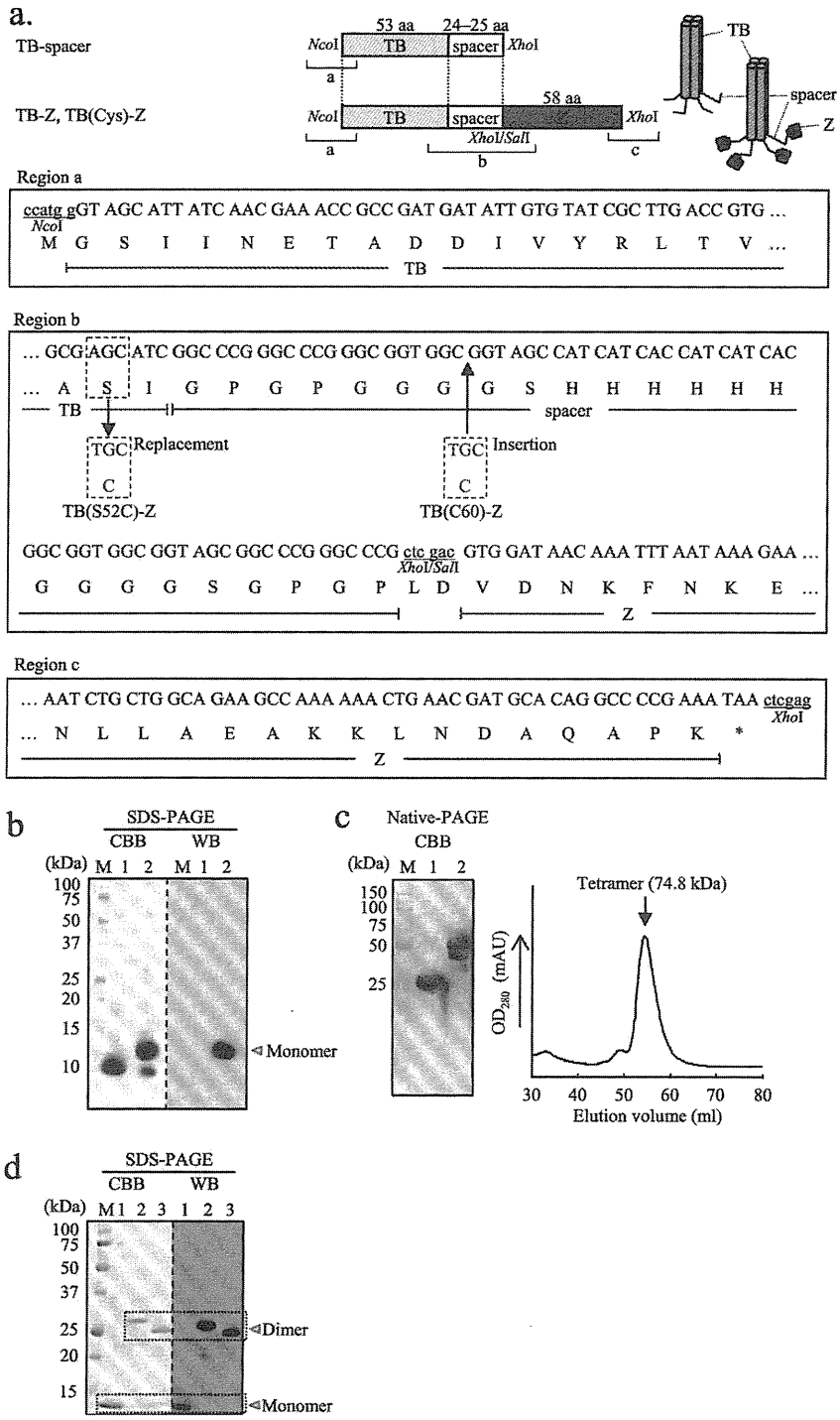

FIG. 1. Expression of the TB-based delivery molecules. (a) Schematic drawing of the tetrabrachion (TB)-derived coiled-coil domain-based constructs: TB-spacer, the TB coiled-coil domain fused to a spacer sequence; TB-Z, TB-spacer fused to the Z domain; TB(Cys)-Z, TB-Z into which a cysteine (Cys) residue has been introduced. The nucleotide and predicted amino acid sequences of the 5′-terminal, junction, and the 3′-terminal regions are shown as regions a, b, and c, respectively. All constructs were cloned between the NcoI and XhoI sites of pET-21d. TB(S52C)-Z is a TB(Cys)-Z in which a Cys was substituted for Ser52 within the coiled-coil domain to introduce a sulfhydryl group for chemical conjugation (as indicated in region b). TB(C60)-Z is another TB(Cys)-Z with a Cys insertion at amino acid position 60 within the hinge region (as indicated in region b). (b and c) SDS-PAGE (b) and native PAGE (c) (left) of the affinity-purified TB-spacer (lanes 1) and TB-Z (lanes 2) and size exclusion chromatography of the TB-Z (c) (right). The protein bands were either stained with Coomassie brilliant blue (CBB) or subjected to Western blotting (WB). (d) SDS-PAGE of the affinity-purified TB-Z (lanes 1), TB(S52C)-Z (lanes 2), and TB(C60)-Z (lanes 3). M, molecular mass marker. The protein bands were either stained with CBB or subjected to WB. For WB (panels b and d), HRP-conjugated goat IgG was applied directly to the blotted membrane for detection of the Z domain-containing proteins.

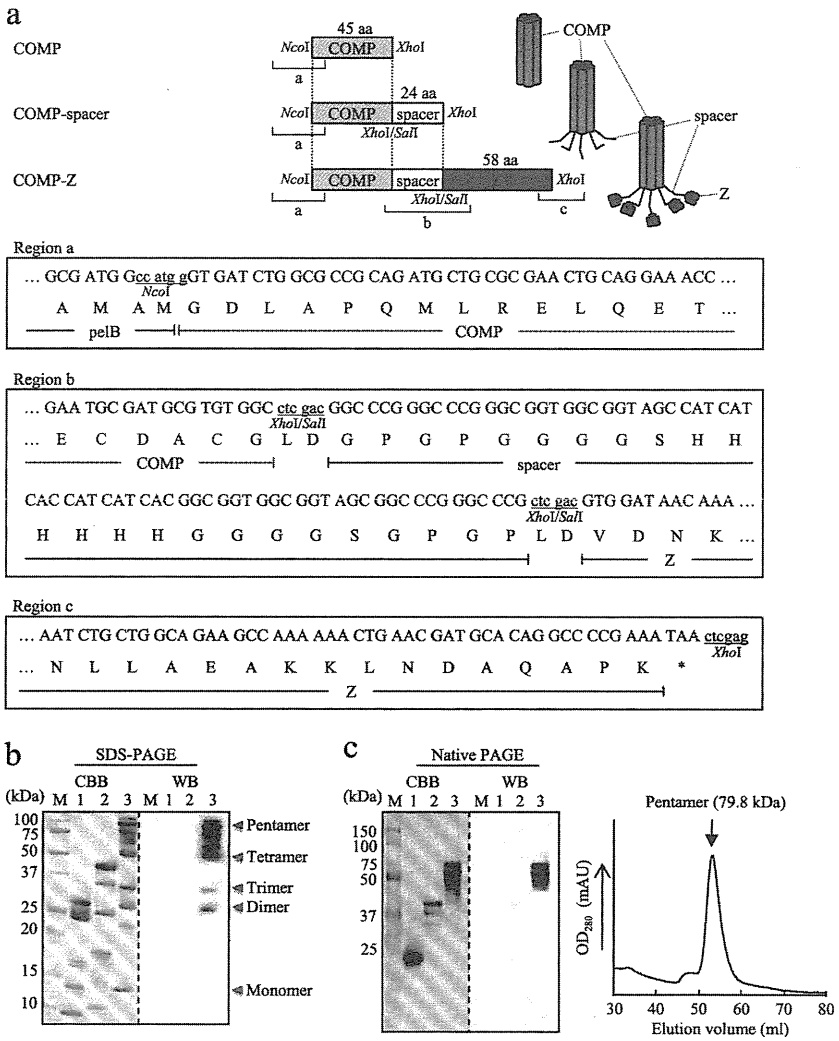

FIG. 2. Expression of the COMP-based delivery molecules. (a) Schematic drawing of the rat cartilage oligomeric matrix protein (COMP)-derived coiled-coil domain-based constructs: COMP, COMP coiled-coil domain; COMP-spacer, COMP fused to a spacer sequence; COMP-Z, COMP-spacer fused to the Z domain. All constructs were cloned between the NcoI and XhoI sites of pET-22b and were expressed as *pelB* fusion proteins. The nucleotide and predicted amino acid sequences of the 5′-terminal, junction, and the 3′-terminal regions are shown as regions a, b, and c, respectively. Two inherent Cys residues within the COMP coiled-coil domain (as indicated in region b) are specific sites used for chemical conjugation. (b and c) SDS-PAGE (b) and native PAGE (c) (left) of the affinity-purified COMP (lanes 1), COMP-spacer (lanes 2), and COMP-Z (lanes 3) and size exclusion chromatography of the COMP-Z (c) (right). M, molecular mass marker. The protein bands were either stained with Coomassie brilliant blue (CBB) or subjected to Western blotting (WB). For WB, HRP-conjugated goat IgG was applied directly to the blotted membrane for detection of the Z domain-containing proteins.

Rodent malaria parasite infection and parasitemia determination. C57BL/6 mouse erythrocytes parasitized by the lethal *P. yoelii* 17XL strain were inoculated i.p. into female C57BL/6 mice (1×10^4 parasitized RBCs/mouse). At various times after inoculation, parasitemia in peripheral blood was monitored by microscopy on Giemsa-stained thin blood smears.

Statistical analysis. The Wilcoxon-Mann-Whitney test was performed to compare antibody titers, or the number of oocysts per mosquito, between the nonimmune control group and a particular immunization group, or between two immunization groups. The Kruskal-Wallis test was performed to compare antibody titers, or the number of oocysts per mosquito, among particular groups. The chi-square test was performed to analyze the difference in the proportion of parasite-free mosquitoes among the total number of mosquitoes examined between the nonimmune control group and a particular immunization group, or between two immunization groups. Kaplan-Meier analyses with the log rank test were performed to compare the survival rates for *P. yoelii*-infected mice between the PBS control group and a particular immunization group. All statistical analyses were conducted with JMP software, version 8.0 (SAS Institute Inc., Cary, NC).

RESULTS

Expression of delivery molecules. The expression of the TB-based constructs, i.e., the TB-spacer and the TB-Z (Fig. 1a), was analyzed (Fig. 1b to d). *E. coli* cultures, including culture supernatants and cell extracts, were subjected to SDS-PAGE. The proteins were detected mainly in the culture supernatants, even though they lacked the leader peptide. Interestingly, the TB constructs fused to the *pelB* signal sequence were not expressed, for unknown reasons. The secreted proteins were

conveniently purified by Ni-NTA chromatography. The affinity-purified TB-spacer and the TB-Z appeared on SDS-PAGE as protein bands with molecular masses of approximately 10 kDa and 12 kDa, respectively (Fig. 1b, CBB). Since the molecular masses predicted from the primary structures of the TB-spacer and TB-Z were 9.2 kDa and 14.9 kDa, respectively, the bands we observed presumably represented their monomers. In contrast, protein bands that were predicted tetramers of the TB-spacer and TB-Z were observed by native PAGE (Fig. 1c, left). In addition, size exclusion chromatography of the TB-Z showed a single chromatographic peak with an estimated molecular mass of 74.8 kDa (Fig. 1c, right), which appeared substantially higher than its calculated mass (i.e., 59.6 kDa for the tetramer). This discrepancy may be attributed to the long rod-like structure of the TB coiled-coil domain, because such molecules generally appear higher in molecular mass than globular proteins of the same mass. These results indicated that the TB-based constructs were secreted from recombinant *E. coli* predominantly as tetramers but were disassembled into monomers in the presence of SDS. The TB-Z, but not the TB-spacer, was shown to bind to the Ig molecule (Fig. 1b, WB).

Next, Cys residues were introduced into the wild-type sequence of the TB-Z for use as a specific antigen-coupling site, because no Cys residues existed within the TB and Z protein moieties. Three candidate sites were selected for Cys insertion. Two of these sites represented Ser substitutions (Ser3 and Ser52), which were chosen out of the four possible Ser residues (Ser3, Ser26, Ser47, and Ser52) because of their presumed degree of side chain exposure to the surface of the coiled-coil domain, based on the 3-dimensional (3D) crystal structure (PDB accession no. 1YBK), and one site represented *de novo* Cys insertion based on the presumed molecular flexibility within the spacer region. Thus, three TB-Z constructs containing Cys residues [TB(Cys)-Z] were engineered: TB(S3C)-Z, TB(S52C)-Z, and TB(C60)-Z. The TB(S3C)-Z construct failed to be expressed in any cellular compartment or in the culture supernatant, but the TB(S52C)-Z and TB(C60)-Z constructs (Fig. 1a, region b) were fully expressed in the culture supernatant, as observed for parental TB-Z, and were purified by Ni-NTA chromatography. For the affinity-purified TB(Cys)-Z [TB(S52C)-Z and TB(C60)-Z], but not for the TB-Z, dimers were observed as predominant molecular species by SDS-PAGE analysis (Fig. 1d, compare lanes 1 with lanes 2 and 3), indicating that disulfide bonds formed between the two subunit pairs within the tetramer. The TB(Cys)-Z could also bind to the Ig molecule, as seen for the TB-Z (Fig. 1d, WB).

COMP-based constructs, i.e., the COMP, COMP-spacer, and COMP-Z, were also engineered (Fig. 2a) and analyzed for their expression in *E. coli*. All three constructs were expressed in culture supernatants similarly to the TB-based constructs. They were purified by Ni-NTA chromatography and were subjected to SDS-PAGE and native PAGE (Fig. 2b and c). Unlike the TB-based proteins, the COMP-based proteins appeared as several bands of various molecular masses under denaturing conditions (Fig. 2b). However, by native PAGE, they appeared predominantly as pentameric forms (Fig. 2c, left). Only the COMP-Z bound to the Ig molecule (Fig. 2b and c, WB). A single chromatographic peak was observed for the COMP-Z by size exclusion chromatography (Fig. 2c, right); its estimated

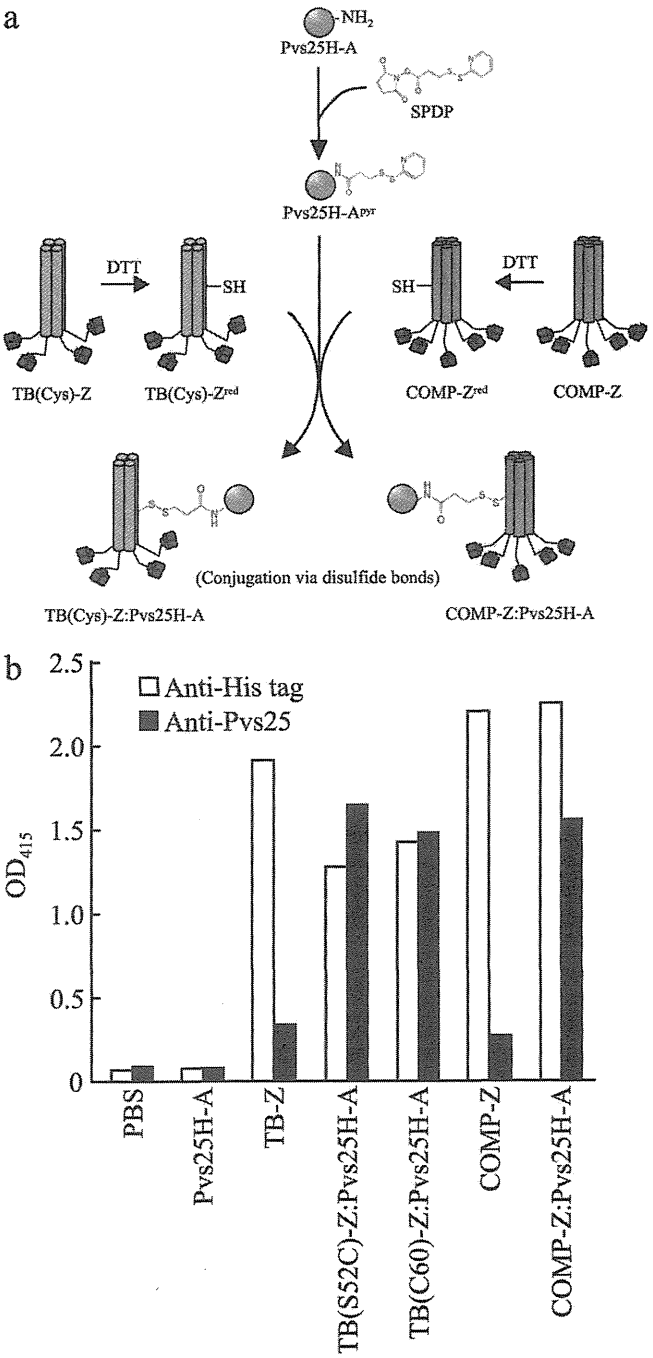

FIG. 3. Chemical conjugation of Pvs25H-A to TB(Cys)-Z [TB(S52C)-Z or TB(C60)-Z] or COMP-Z. (a) Chemical conjugation scheme for the construction of the TB(Cys)-Z:Pvs25H-A and COMP-Z:Pvs25H-A tricomponent complexes. The heterobifunctional cross-linker *N*-succinimidyl-3-(2-pyridyldithio)propionate (SPDP) was used to link the Pvs25H-A antigen (22) to the TB(Cys)-Z or COMP-Z delivery molecule via disulfide bonds. The delivery molecules were first treated with dithiothreitol (DTT) to expose free sulfhydryls [designated TB(Cys)-Z^{red} or COMP-Z^{red}], and then pyridyldithiol-activated Pvs25H-A (Pvs25H-A^{pyr}) was reacted with the delivery molecules to generate the tricomponent complexes. (b) The complexes generated were analyzed by a human IgG-ELISA using an anti-His (open bars) or anti-Pvs25 (filled bars) antiserum.